Minerals Engineering 218 (2024) 108993

Contents lists available at ScienceDirect

Minerals Engineering

journal homepage: www.elsevier.com/locate/mineng

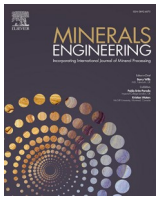

Geometallurgy of the Tenke-Fungurume sediment-hosted copper-cobalt district, D.R. Congo

Isabel F. Barton [a,*], Robert M. North [b]

[a] Department of Mining & Geological Engineering, University of Arizona, Tucson, AZ, USA
[b] Formerly with CMOC, Phoenix, AZ, USA

ARTICLE INFO

Keywords:
Tenke-Fungurume
Geometallurgy
Cu-Co deposits
Process mineralogy
Central African Copperbelt

ABSTRACT

This paper presents and analyzes the geometallurgy of ores at the Tenke-Fungurume district, a major global source of Cu and Co. Ores at depth are mainly Cu, Cu-Fe, and Cu-Co sulfides (chalcocite group, chalcopyrite, bornite, carrollite, pyrite) hosted in variably silicified dolomite and shale layers. Within roughly 200 m of the surface the sulfides are overprinted by malachite, heterogenite, brochantite, pseudomalachite, and chrysocolla. A mixed zone at intermediate depth contains metals as cobaltoan dolomite, sphaerocobaltite, cuprite, and native copper in addition to sulfides and oxides (*sensu lato*).

Geometallurgical properties are highly variable and anisotropic due to the wide unit-to-unit variation in lithology and alteration. Average crusher work index varies from 6.3 to 8.6 kWh/t across units. Average grinding Bond work index ranges from 10.8 kWh/t in the basal argillaceous conglomerate to 15.4 kWh/t in the overlying, variably silicified dolomitic shales. In these dolomitic shales, both work indices correlate strongly with rock uniaxial compressive strength. The same correlation is present in an unlaminated silicified algal dolomite, in which abrasion index also correlates with quartz content. There are no other observed correlations among comminution characteristics, geomechanical properties, and mineralogy.

Flotation tests show average recoveries of 87% Cu and 61% Co in the sulfide stage, 61% Cu and 40% Co in the oxide stage. Highest recoveries came from the variably silicified dolomitic shales, the lowest from the extremely phyllosilicate-rich basal unit. The main losses in flotation are of oxide minerals and some chalcocite. Apart from the rejection of cobaltoan dolomite, most flotation problems are due to muscovite, biotite, and chlorite, which report to concentrate and may cause sliming and other sources of loss.

Leach test recoveries for Cu and Co show strong inverse correlations with the fraction of metal hosted in sulfides. Oxide-dominated ores are generally 80–90 % leachable, with Cu recoveries < 20 % for primary sulfides other than chalcocite. In leach testing, Co recoveries exceed Cu recoveries in the same samples, though ultimate Co recovery in practice is lower due to more locking and minor Co hosted in insoluble chlorites. Acid consumption is a function of dolomite concentration and varies from a low of 226 kg/t in a slightly dolomitic shale to a high of 435 kg/t in a laminated dolomite. Acid consumption by other gangue minerals is undetectable over the timescale of testing.

Ores are divided into one of six types at the mine: sterile; leached; oxide; sulfide; oxide-dominant mixed; and sulfide-dominant mixed ores. The first two of these are below cutoff grade and contain few or no Cu or Co minerals. Higher-grade material is subdivided into the last four categories based on results from quick-leach testing and 1-hour acid-soluble Cu analysis, along with logged mineralogy. Overall, the main controls on geometallurgical behavior are (1) depth below surface, which influences grade and determines ore mineral type and leachability, and (2) rock type, which affects comminution and flotation characteristics and acid consumption. Many of the results highlight the need for geometallurgical characterization to include as much textural and geological information as possible to aid in correlating geological features with metallurgical outcomes.

* Corresponding author.
E-mail address: fay1@arizona.edu (I.F. Barton).

https://doi.org/10.1016/j.mineng.2024.108993
Received 19 May 2024; Received in revised form 10 September 2024; Accepted 11 September 2024
Available online 22 September 2024

1. Introduction

As the world's population grows and technology advances and spreads, the need for metals rises. Two of the most necessary are copper (Cu) and cobalt (Co), used respectively in electrical wiring (Cu) and in batteries and steel (Co). Sediment-hosted Cu-Co deposits produce a small but significant fraction of global Cu and about two-thirds of global Co each year.

Despite their importance to global materials supplies, sediment-hosted Cu-Co deposits remain under-studied. A particular blank spot in the literature is their geometallurgy, or how the sediment-hosted Cu-Co deposits' mineralogy and geology relate to the outcomes of metallurgical processing. While geometallurgical studies add considerable value to mining, they are rare for this deposit type, and few such studies on any deposit consider large-scale data across most or all parts of processing and metallurgy (e.g. Coward et al., 2009; Boisvert et al., 2013; Little et al., 2018; Lotter et al., 2024). This paper aims to provide a holistic overview of the geometallurgy of one of the most important such deposits, including its mineralogical and geological characteristics and their effects on metallurgical results.

1.1. Overview of the Tenke-Fungurume district

Tenke-Fungurume is one of the world's foremost Cu deposits with over 68 billion pounds (31 million metric tons, Mt) of contained Cu resources at an average grade estimated at 2.26 wt% Cu as identified by the CMOC Group (CMOC Annual Report 2022). It contains over half the world's known Co reserves, with over 3.5 million tonnes Co in identified resources (CMOC Annual Report, 2022). Tenke-Fungurume lies within the Central African Copperbelt, which stretches over 600 km roughly following the Zambia-DR Congo border from Ndola, Zambia in the southeast to its apex near Tenke-Fungurume and continuing southwestward through Kolwezi and into Angola. The Central African Copperbelt is the largest Cu- and Co-producing area in Africa and one of the most important Cu and Co regions in the world.

The Tenke-Fungurume district consists of over 150 separate mineralized tectonic blocks, grouped into 35 named deposits which were drilled by Freeport-McMoRan between 2006 and 2016 (Fig. 1). The named areas extend approximately 35 km east–west and 9 km north–south and contain between 1 and 15 separate structural blocks. Metal resources have been estimated from geologic modeling of 15 deposits and groups of deposits.

1.2. Geologic background to the geometallurgy of Tenke-Fungurume

1.2.1. Areal, depth, and stratigraphic patterns

Ores are hosted in the Mines Series, a stack of mainly dolomite and shale units dating from the Proterozoic (described in detail by Schuh et al., 2012). The district consists of scattered rafts or "écailles" of this Mines Series in various shapes and states of mineralization (Fig. 1). Écailles are typically 100 m to 1 km long and terminate in faults. Richly mineralized, poorly mineralized, and barren écailles occur throughout the district, without apparent correlation with any large-scale geological features (Fay, 2014).

Depth below the modern surface exercises a strong control on the nature and grade of mineralization (Fig. 2). In the 10 m or so nearest the surface, metals have generally been leached from their Mines Series hosts by supergene alteration, removing Cu and reducing Co contents to a subeconomic "cobalt cap" generally grading < 0.05 % Co (Fay and Barton, 2012). The host mineral in the cobalt cap is uncertain, likely extremely low-grade heterogenite and/or minor Co substitution in Fe and Mn oxides. Below this, supergene oxides dominate down to 50 or 100 m depending on the location, rock unit, and proximity to faults. The supergene oxides are mostly malachite, heterogenite, and chrysocolla, with accessory pseudomalachite, brochantite, libethenite, plancheite, and cornetite. Below the supergene oxides are the mixed ores (Fig. 2). Over this zone the supergene oxides on top are gradually supplanted by cuprite, cobaltoan dolomite, native copper, and chalcocite. The proportion of chalcocite increases downward as the mixed zone grades into the sulfide zone, primary ores consisting of chalcocite, bornite, chalcopyrite, and carrollite. The boundary between the mixed and sulfide zones is rarely a sharp gradation and its depth varies, but 200–300 m below the surface is typical.

Ore grade and ore and gangue mineralogy also show a strong stratigraphic control (Fig. 3, Table 1). Most of the Cu-Co grade is hosted in two laminated strata (SDB and RSF-DStrat) above and below a massive

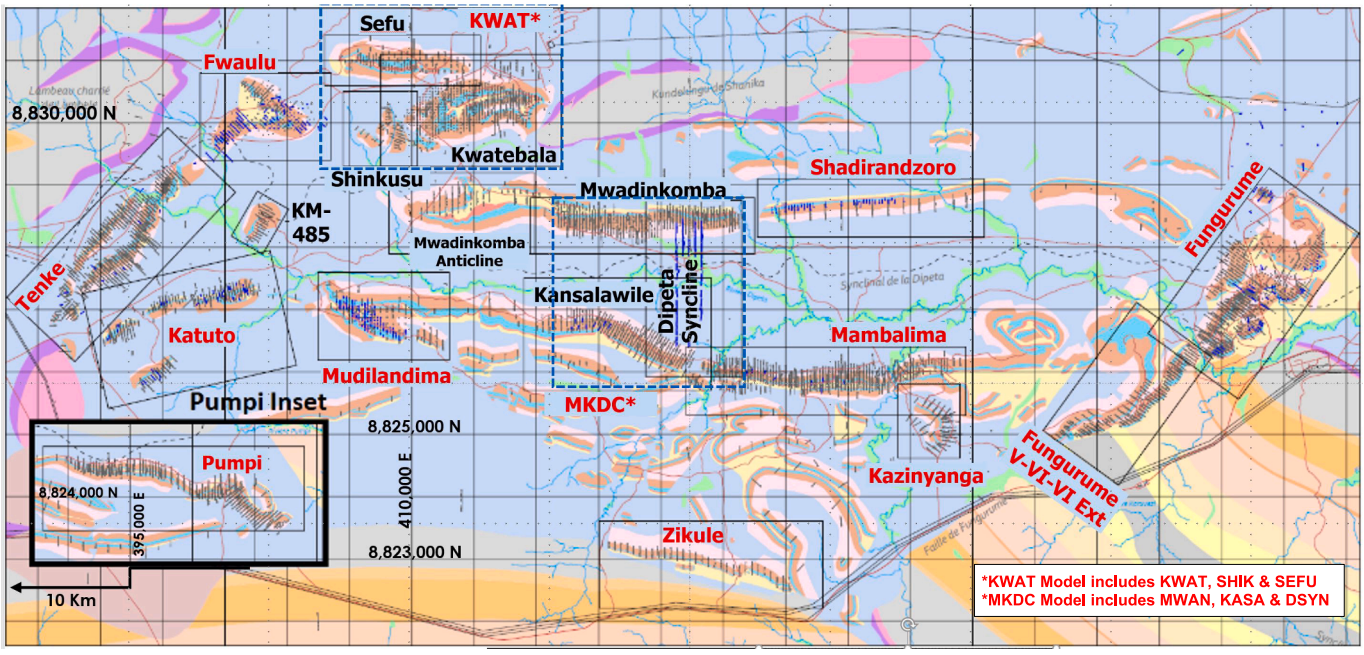

Fig. 1. Distribution of mineral deposits in the Tenke-Fungurume copper-cobalt concession showing geological resource-model boundaries. Model names in red are those used in planning and calculating reserves as reported in the CMOC Annual Report 2022.

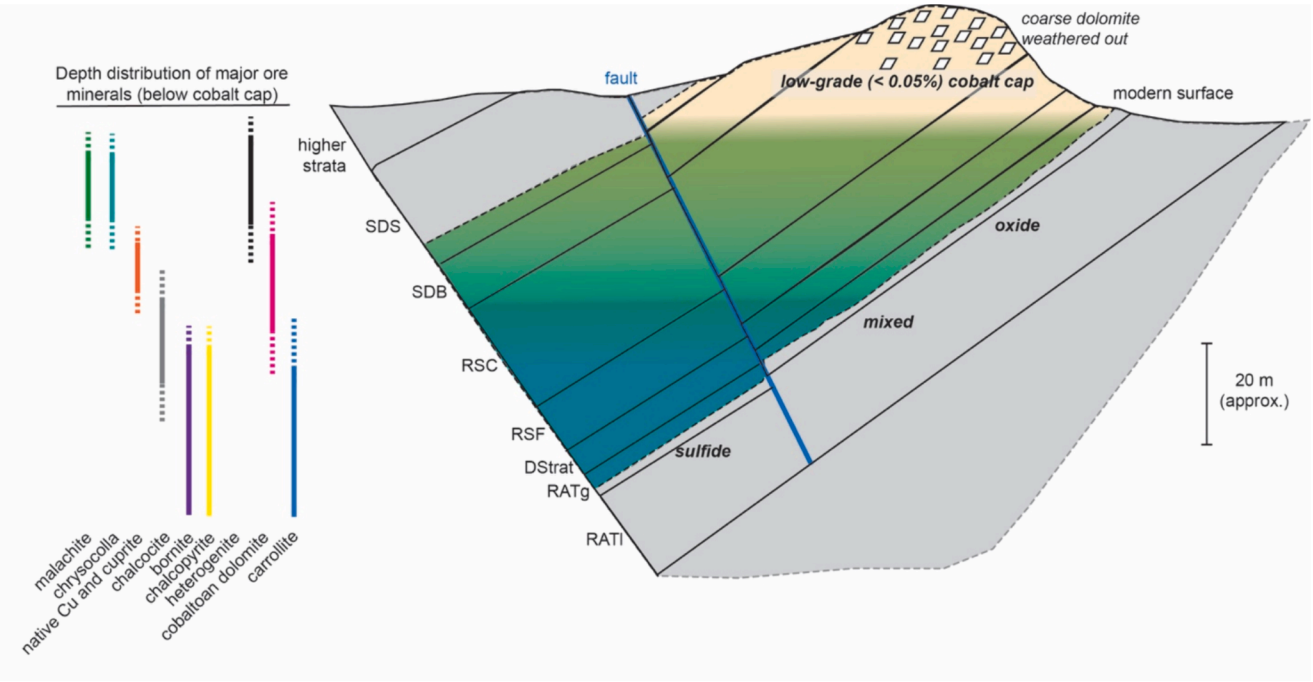

Fig. 2. Schematic gradation from near-surface leached rock to oxide, then mixed, then sulfide ores with depth. Mixed-sulfide boundary is not to scale. See Table 1 and section 1.2.2 for formation names.

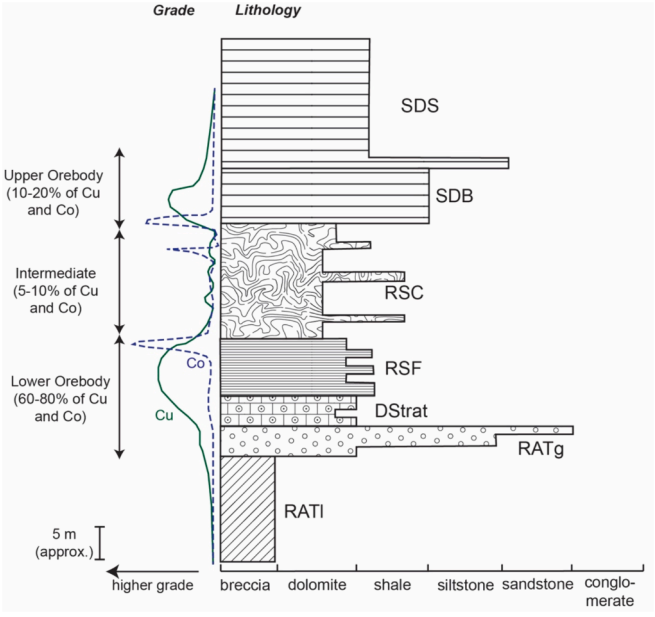

Fig. 3. Approximate stratigraphic column of the Mines Series at Tenke-Fungurume. Lithology varies from place to place. See text for discussion and Table 1 for rock formations.

dolomite with lower, though usually still economic, grades.

1.2.2. *Descriptive mineralogy and composition of each unit*

The important copper and cobalt production is from the lower Mines Series Sub-Group of the Roan Group, locally known as the Mines Series at TFM and broken out into specific formations as shown in Table 1 and Fig. 3. Upper units are devoid of economic copper-cobalt mineralization. Below are general descriptions and sedimentological interpretations with emphasis on implications for geometallurgy.

R-1 RAT (Roches Argilo-Talqueuses, clay-talc rocks): The oldest outcropping (and drilled) unit at TFM is the RAT, traditionally interpreted as oxidized fill in an incipient continental rift basin with inferred (not now existing) original evaporite beds (Jackson et al., 2003 and references therein). The entire R-1 sequence has been referred to as "RAT lilas" or purple RAT (Francois, 1987) due to its reddish to purple color from fine-grained hematite.

Table 1
Lithology and stratigraphy of the Mines Series at Tenke-Fungurume. See text below for full names of formations.

Unit	Dominant rock type, texture, and alteration
R-2.2.2 to R-2.2.3 SDS	Finely laminated (dolomitic) shales and massive dolomites
R-2.2.1 SDB	Finely laminated dolomitic shales, minor silicification
R-2.1.3 RSC	Silicified fenestral algal dolomite
R-2.1.2.2 RSF	Finely laminated, variably silicified dolomitic shales
R-2.1.2.1 DStrat	Finely laminated dolomite > shale, minor silicification
R-2.1.1 RAT gris	Gray argillaceous & dolomitic siltstones & sandstones
R-1 RAT lilas	Red argillaceous, dolomitic siltstones above (pseudo)-breccias

The lower RAT includes oxidized breccia with fine-grained sandstone and siltstone. Total thickness is unknown but inferred to exceed 200 m; however, only the top 1–15 m are included in the Mines Series (discussed by Schuh et al., 2012). Its thickness varies inversely with the extent of folding and faulting in the area. In intensely disrupted areas the RAT lilas varies from zero to a few m thick; in gently folded zones it is consistently 10–15 m (Fig. 4). The unit is typically porous and thus mineralized up to 0.25 % Cu with malachite, ancillary chrysocolla, and rare chalcocite in the oxide (supergene) zone, probably transported from the overlying higher-grade units. Magnesian chlorite and quartz are identified as the major gangue minerals in detailed studies.

R-2.1.1 RAT gris (Gray RAT). RAT gris forms the base of the Kamoto Dolomite (Bartholomé et al., 1973). It can be mineralized at > 0.25 % Cu, mainly with malachite and rare chrysocolla in the oxide zone. Deeper drilling showed chalcocite > bornite > chalcopyrite in primary mineralization. It is worth noting, however, that the RAT gris may contain mixed or oxide (malachite) ores below sulfide mineralization in

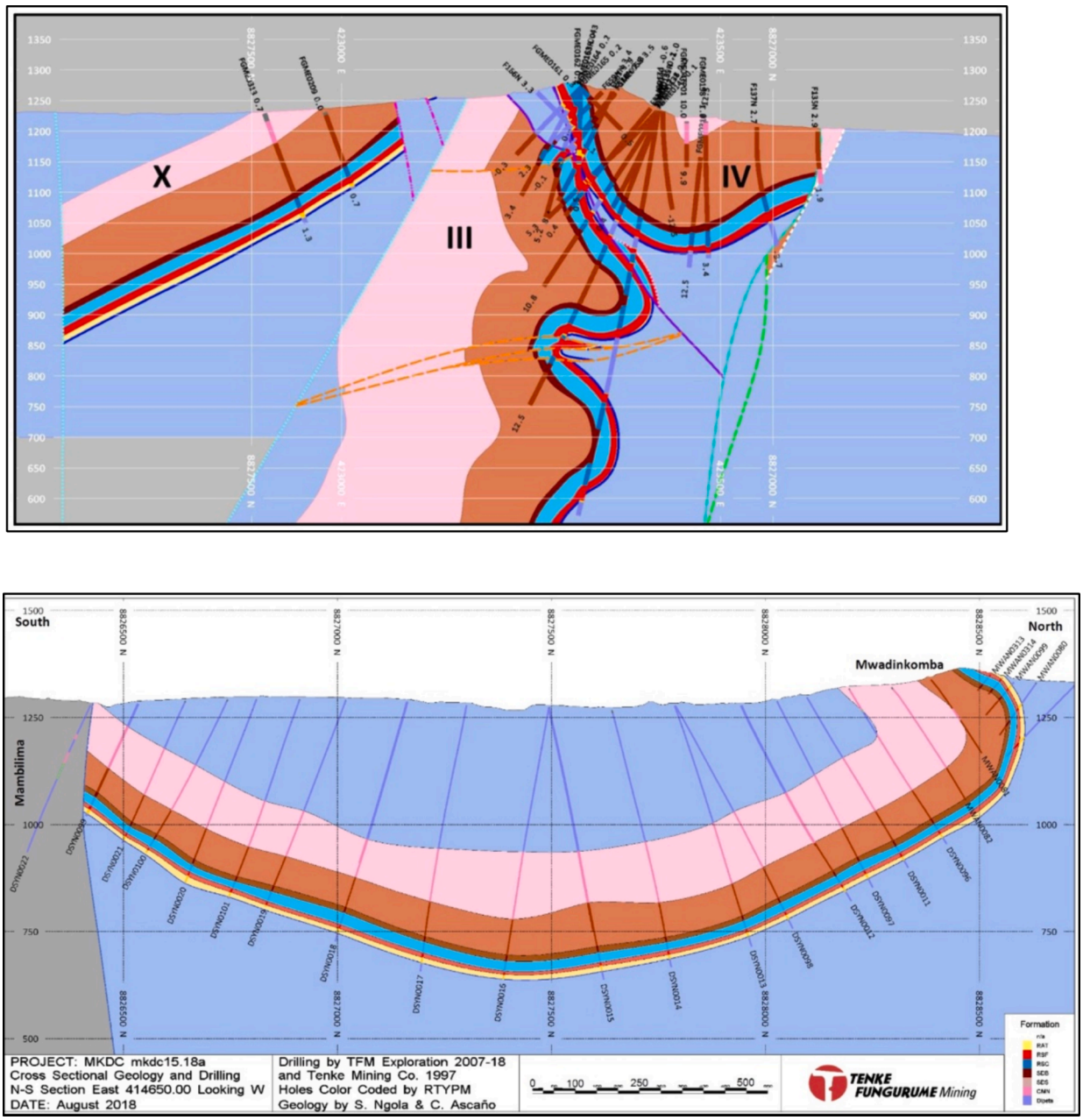

Fig. 4. Variably complex structures of the Mines Series Subgroup at Tenke-Fungurume. Top, complex folds and faults repeat strata and juxtapose units of the Lower Orebody against the Dipeta Subgroup around Fungurume deposits III and IV. Bottom, a simple synclinal structure in the Mwadinkomba écaille. See Fig. 1 for locations.

the overlying units, indicating a different flow regime during supergene alteration. Like the RAT lilas, mineralogy and assays based on a limited number of samples indicates the main gangue minerals are Mg-chlorite and quartz.

R-2.1.2.1 DStrat (Dolomites Stratifiées, stratified dolomites). The DStrat conformably overlies RAT gris and is grouped with the lithologically similar, overlying RSF in the TFM geological interpretations. The unit is consistently 2.5–3.5 m thick across the concession and consists of a relatively thick-bedded dolomite (Schuh et al., 2012).

Logged copper mineralogy in DStrat in the oxide zone is malachite with subordinate chrysocolla. Primary sulfide minerals include chalcocite, bornite, chalcopyrite, and carrollite. Gangue mineralogy is dominantly dolomite with significant quartz. Chlorite is noted in all detailed analyses, at times exceeding 20 %. Copper grades are high, averaging around 3 %, with only the RSF being higher-grade. Cobalt grades average about 0.20 % but are highly variable.

R-2.1.2.2 RSF (Roches Siliceuses Feuilletées, laminated siliceous rocks). RSF conformably overlies DStrat and is distinguished by its finely laminated bedding and higher ratio of siliciclastic to dolomitic components. Its chemistry is generally reducing, with organic constituents (no longer existing) that probably provided the reductant needed for ore formation. The unit is typically silica-rich, partly due to an influx of Si during alteration, and published accounts give ranges of 31 to 86 % SiO_2 (Kampunzu et al., 2005; Fay and Barton, 2012). Whole-rock geochemistry on 499 RSF samples from Kwatebala averaged 56.5 % SiO_2, ranging from 12 to 92 %. Typical thickness is about 8 m, with structurally simple areas such as the Dipeta Syncline averaging closer to 7.5 m.

The RSF represents the most important ore host throughout the district. With the DStrat, it is nearly always at ore grade in mineralized écailles: historically oxide-zone RSF can reliably be sent to the plant

without assays. Drilling in the Dipeta Syncline and bulk sampling at Fungurume and Kwatebala suggest that the same is true of sulfide material in the RSF. Weakly mineralized material is known in drilling in distal parts of the Fungurume area, specifically Fungurume XV (Fig. 1), but exceptions are rare. Otherwise the RSF is below ore grade only where the entire host écaille is unmineralized.

In early geologic modeling, the RSF was considered together with the RAT Gris, DStrat, and sometimes lower RSC in a single unit called the "Lower Orebody." Detailed evaluation of chemical analyses from extensive drilling by TFM, however, demonstrates that the units are statistically distinctive enough in metallurgical behavior to consider them individually. This is especially true at the contact between RSF and overlying RSC, where copper grade decreases rapidly from an average of 3.2 % in RSF to $>$ 0.5 % in the RSC above. Typically cobalt grades are highest in RSF near the contact with RSC.

Malachite has historically been the most important copper-bearing mineral in RSF, produced in the oxide zone at TFM and extending through the Dipeta Syncline mixed zone to depths down to 380 m. Chrysocolla is next most significant. Sulfide mineralogy includes chalcocite, bornite and chalcopyrite, in order of relative importance, zoning stratigraphically outward from the RSC suggested from observations in the bulk-sampling workings at Kwatebala.

R-2.1.3 RSC (Roches Siliceuses Cellulaires, cellular siliceous rocks). The top of the RSF is a conformable but highly abrupt contact with the overlying RSC. At depth the RSC consists of mixed silica and dolomite, but near the surface the dolomite is weathered out to leave a resistant ridge consisting of silica with holes up to 10 cm diameter where the dolomite used to be. Intercalated shale layers of up to 2 m width and several 10 s of meters extent along strike and down-dip are common, often localizing higher-grade mineralization. Thickness of the RSC ranges from 20 to 30 m, averaging about 23 m in the absence of major deformation.

Mineralization in the RSC is typically low-grade, contrasting with the RSF below and SDB above. In the oxide zone malachite dominates, compared to chalcocite in the sulfide zone. Cobaltoan carbonates, mainly cobaltoan dolomite and spherocobaltite (Barton et al., 2014), are the most common cobalt minerals in the oxide and mixed zones; carrollite is the only Co-bearing sulfide. Rims of heterogenite surround carrollite in the transition from the oxide to sulfide zones.

R-2.2.1 SDB (Schistes Dolomitiques du Base, basal dolomitic shales). A series of dolomitic shales above the Kamoto Formation represents a change from laminated dolomites (RSF) to reef dolomites (RSC) to dominantly clastic sediments. These dolomitic shales are together are referred to as the SD, Schistes Dolomitiques, R-2.2 and can be subdivided into three major subdivisions over about 110 m (Cailteux, 1994). Logging at TFM typically applied two subdivisions, a lower (often mineralized) SDB or Schistes Dolomitiques du Base and an upper SDS, Schistes Dolomitiques Superieures. The contact between SDB and SDS is marked by the first dolomite-cemented sandstone in the sequence. Often, the SDB has high cobalt grades in the first few meters above the RSC, but grade decays rapidly up-section. Dolomite-quartz nodules (replacing gypsum) are common, often rimmed by diagenetic pyrite $\pm$ chalcopyrite in unoxidized examples. Drilling in the Dipeta Syncline suggests an average thickness of about 12.5 m for SDB.

Primary mineralization in SDB consists of chalcopyrite with pyrite also common, in contrast to the higher metal:sulfur ratios of other units. This results in a weathering pattern that causes Cu, though less Co, to leach from the SDB during weathering. Partially leached SDB has been noted with copper remaining as an insoluble oxide as yet unidentified. This material averages about 0.25 % TCu, often with no copper mineral logged.

R-2.2.2, R-2.2.3 SDS (Schistes Dolomitiques Supérieures, upper dolomitic shales). Dolomitic shales continue above the SDB and have been subdivided into several units (Cailteux, 1994) that can often be identified in core logging but are typically lumped together. Mineralization is intermittent but in some places reaches ore grade. The SDS is typically between 75 and 90 m thick at TFM, but with a range from 60 to 110 overall. Drilling in the Dipeta Syncline averaged 70 m with chalcopyrite mineralization averaging 0.07 % total copper.

The SDS commonly reaches ore grade in the oxide zone but in small tonnages. High-grade malachite is seen occasionally but overall the unit is not an important ore host. Pyrite and chalcopyrite are commonly noted in the sulfide zone, as with the SDB but typically lower grade. Units above the SDS are not considered ore-bearing.

Mineralogical summary for the Mines Series. Table 2A summarizes the modal mineralogy of each unit in the sulfide, oxide, and mixed zones in the principal ore-bearing units. More detailed breakdowns of average Cu and Co deportment by unit are shown in Tables 2B-2C. Finally, Table 2D offers a summary of mineral association data for the Cu and Co sulfides at Tenke-Fungurume.

1.3. Metallurgical overview

The Tenke-Fungurume district has produced Cu cathode and Co hydroxide precipitate since March 2009. Ores are mined and trucked to three grinding circuits consisting of a pebble crusher and a SAG mill each. After grinding, ores are leached in agitated tanks at ambient temperature with sulfuric acid, adding sodium metabisulfite ($Na_2S_2O_5$) as a reducing agent. This reduces Fe^{3+} to Fe^{2+}, which reduces the Co^{3+} in heterogenite to the soluble Co^{2+} state for extraction. Leach solutions are sent to Cu solvent extraction and electrowinning. Cobalt is extracted from the raffinate by precipitation with MgO at 45 ℃ and pH of 7.5 (Crundwell et al., 2020). Reported production for 2022 was approximately 21,600 metric tons Co and 280,300 metric tons Cu (CMOC Group Limited 2023 Annual Report, p. 2). Overviews of parts of the extractive processes at Tenke-Fungurume and related Copperbelt deposits are available from Sandoval et al. (2016), Lee and Wellington (2017), Alexander et al. (2018), Sole et al. (2019), Crundwell et al. (2020), and others.

1.4. Motivation for this paper

Published information about the Tenke-Fungurume district is surprisingly scarce considering its importance to the global metals supply. The same is true of sediment-hosted Cu-Co deposits in general: the literature about them is scanty compared to other deposit types, and what exists is mainly geological. A few papers and proceedings contributions cover individual aspects of the metallurgy at particular Copperbelt deposits. Sandoval et al. (2016) described the updates to the electrowinning circuits at TFM. Little et al. (2018) related flotation recovery to ore mineralogy in the mill at Kansanshi, finding that highest recoveries were obtained from sulfide minerals and the lowest from floating oxides. Lotter et al. (2024) implemented process mineralogy studies at Kamoa and Kakula, describing sampling and testing methods that successfully scaled up laboratory processes to the operating plant. But to date there have been few systematic, data-based overviews of the geometallurgy or process mineralogy of sediment-hosted Cu-Co deposits or of the important TFM district.

More generally, there are also few papers in the geometallurgical literature that combine extensive metallurgical and geological datasets to examine the geometallurgy of a deposit at the production scale and through all stages of processing. With few exceptions (e.g. Boisvert et al., 2013; Preece et al., 2023), most studies attempting to link mineralogy to metallurgical performance have thus been limited to a small (laboratory) scale, to a small part of the metallurgical process, or to inference and hypothesis. This paper attempts to uncover geology-metallurgy connections through a data-driven approach that spans the full range from geology through extraction.

2. Materials and methods

The datasets used here were compiled from metallurgical tests

Table 2A
Average grades and mineralogical compositions of the Mines Series rocks, in weight percents. Values shown are overall averages ± 1 standard deviation, mainly for mixed and sulfide ores, from The 46 samples taken in 2013 (see Table 3). RAT data are not shown due to a low number of samples.

Chemical assays	SDB	RSC	RSF	DStrat
% Co	0.53 ± 0.49	0.49 ± 0.48	0.22 ± 0.24	0.13 ± 0.20
% Cu	3.57 ± 2.46	2.26 ± 1.90	4.44 ± 1.61	3.80 ± 2.42
Modal mineralogy by QEMSCAN				
Chalcopyrite	1.04 ± 1.32	0.01 ± 0.02	0.30 ± 0.54	0.23 ± 0.52
Chalcocite	2.61 ± 2.59	1.93 ± 2.20	3.09 ± 2.39	3.10 ± 2.31
Bornite	0.37 ± 0.84	0.06 ± 0.08	2.03 ± 1.55	1.74 ± 2.44
Covellite	0.31 ± 0.28	0.04 ± 0.08	0.20 ± 0.12	0.06 ± 0.03
Carrollite	1.02 ± 1.16	0.84 ± 1.02	0.64 ± 0.83	0.38 ± 0.68
Malachite	0.42 ± 0.62	0.64 ± 0.73	0.40 ± 0.93	0.19 ± 0.35
Brochantite	0.24 ± 0.13	0.13 ± 0.12	0.21 ± 0.12	0.16 ± 0.1
Chrysocolla	0.11 ± 0.10	0.07 ± 0.08	0.11 ± 0.18	0.03 ± 0.04
Cu-bearing clays	0.67 ± 0.56	0.13 ± 0.17	0.44 ± 0.33	0.22 ± 0.15
Cu-bearing gangue	0.17 ± 0.16	0.08 ± 0.13	0.41 ± 0.26	0.38 ± 0.26
Cu-bearing iron oxides	0.26 ± 0.31	0.20 ± 0.24	0.14 ± 0.20	0.10 ± 0.12
Cu oxides, undifferentiated	0.01 ± 0.01	0.02 ± 0.05	0.03 ± 0.06	0.01 ± 0.02
Native Cu	0.00 ± 0.00	0.00 ± 0.01	0.01 ± 0.02	0.00 ± 0.02
Other Cu-bearing minerals	0.02 ± 0.02	0.02 ± 0.02	0.04 ± 0.02	0.03 ± 0.01
Heterogenite	0.44 ± 0.91	0.66 ± 0.94	0.05 ± 0.10	0.01 ± 0.02
Co-bearing gangue	0.09 ± 0.13	0.15 ± 0.23	0.01 ± 0.02	0.01 ± 0.01
Cobaltoan dolomite	0.12 ± 0.15	0.23 ± 0.19	0.04 ± 0.11	0.03 ± 0.08
Other Co-bearing minerals	0.24 ± 0.23	0.25 ± 0.32	0.08 ± 0.07	0.03 ± 0.04
Pyrite	0.66 ± 1.00	0.00 ± 0.00	0.00 ± 0.01	0.01 ± 0.02
Quartz	35.36 ± 8.33	55.60 ± 8.06	37.77 ± 7.59	28.44 ± 3.73
K-feldspar	4.42 ± 2.24	0.62 ± 0.85	1.41 ± 1.58	0.12 ± 0.21
Plagioclase	0.01 ± 0.00	0.00 ± 0.00	0.02 ± 0.01	0.01 ± 0.02
Muscovite	19.14 ± 7.94	3.58 ± 4.72	3.98 ± 3.65	0.32 ± 0.63
Chlorite/Biotite	10.83 ± 4.15	3.90 ± 2.48	4.90 ± 2.46	5.81 ± 3.23
Mixed clays (no Cu)	0.38 ± 0.13	0.23 ± 0.18	0.45 ± 0.32	0.65 ± 0.58
Calcite	0.02 ± 0.03	0.07 ± 0.13	0.05 ± 0.07	0.06 ± 0.04
Dolomite (no Co)	19.25 ± 10.82	29.47 ± 10.43	42.28 ± 9.77	57.23 ± 6.50
Iron oxides (no Cu)	0.70 ± 0.72	0.45 ± 0.76	0.23 ± 0.21	0.20 ± 0.27
Other	1.12 ± 0.34	0.59 ± 0.31	0.68 ± 0.22	0.47 ± 0.31

Table 2B
Percentage of Cu hosted in various minerals, average for each Mines Series unit. Values shown are overall averages ± 1 standard deviation, not differentiated by oxide, sulfide, or mixed zone.

Mineral	SDB	RSC	RSF	DStrat
Chalcopyrite	9.87 ± 12.62	0.13 ± 0.15	2.80 ± 5.15	2.17 ± 5.06
Chalcocite	56.18 ± 56.09	42.63 ± 48.44	66.98 ± 52.58	67.19 ± 50.56
Bornite	6.48 ± 14.69	0.96 ± 1.34	35.11 ± 26.87	30.38 ± 42.92
Covellite	4.20 ± 3.77	0.65 ± 1.17	2.64 ± 1.55	0.98 ± 0.61
Carrollite	8.40 ± 9.03	6.56 ± 7.38	4.98 ± 5.70	2.82 ± 4.46
Malachite	6.78 ± 10.00	10.31 ± 11.74	6.40 ± 14.86	3.09 ± 5.58
Brochantite	3.11 ± 1.91	2.11 ± 1.92	2.91 ± 1.99	2.27 ± 1.63
Chrysocolla	1.02 ± 0.99	0.71 ± 0.73	1.06 ± 1.77	0.31 ± 0.42
Cu in heterogenite	0.35 ± 0.75	0.63 ± 1.01	0.05 ± 0.13	0.01 ± 0.02
Cu-bearing clays	0.92 ± 0.83	0.13 ± 0.20	0.45 ± 0.40	0.13 ± 0.07
Cu-bearing gangue	0.79 ± 0.76	0.43 ± 0.71	2.23 ± 1.32	2.25 ± 1.46
Cu-bearing iron oxides	1.00 ± 1.01	0.81 ± 0.94	0.74 ± 0.73	0.55 ± 0.46
Cu oxides	0.18 ± 0.17	0.64 ± 1.25	1.07 ± 1.94	0.24 ± 0.55
Other Cu-bearing minerals	0.71 ± 1.13	2.06 ± 3.81	0.19 ± 0.47	0.03 ± 0.04

Table 2C
Percentage of Co hosted in various minerals, average for each Mines Series unit. Values shown are overall averages ± 1 standard deviation, not differentiated by oxide, sulfide, or mixed zone.

Mineral	SDB	RSC	RSF	DStrat
Carrollite	59.98 ± 73.30	53.61 ± 65.64	38.34 ± 54.69	24.12 ± 45.87
Cobaltoan dolomite	2.32 ± 4.50	1.85 ± 1.44	0.33 ± 0.85	0.20 ± 0.63
Heterogenite	32.11 ± 61.29	55.73 ± 79.47	4.20 ± 9.21	0.85 ± 2.13
Co-bearing gangue	2.20 ± 3.08	3.53 ± 4.13	0.44 ± 0.56	0.15 ± 0.21
Other Co-bearing minerals	3.36 ± 3.30	1.91 ± 1.66	1.18 ± 1.11	0.52 ± 0.63

carried out by Freeport-McMoRan Inc. from 2011 through 2014, two years before the sale of the Tenke-Fungurume district to CMOC. Rock Quality Designation (RQD) and point load tests were carried out on site using geological drill core as part of routine core characterization. RQD was assessed as the percentage of each meter's worth of drill core made up of pieces > 10 cm long. Point load testing was carried out using a GCTS PLT-110 point load tester. Of the point load tests in the dataset, 3,819 were on diametrically oriented core, 18 were axially oriented, and one lacked orientation information. Uniaxial compressive strength (UCS) testing was done by external geotechnical contractors in general accordance with ASTM D7012.

The process samples were either core composites, representing a several-meter interval of drill core within one formation; domain composites representing one stratigraphic unit each; or master composites across all formations (Table 3).

Samples were shipped to Freeport-McMoRan's Technology Center for assay, mineralogical analysis, comminution, flotation, and leach testing.

For all samples, chemical assays were performed by acid digestion and solutions were analyzed by inductively coupled plasma optical emission spectroscopy / mass spectroscopy (ICP-OES/MS) for %Cu, % Co, and 54 other elements. The selection of other elements varied over time; only the 2013 samples were analyzed for Si. Carbon and sulfur speciation were analyzed by Leco. X-ray diffractometry (XRD) and automated mineralogy (QEMSCAN) analyses were carried out at the

Table 2D
Mineral association data for 8 Fungurume sulfide samples from the Lakefield group (see Table 3) at a target grind size of 212 μm (SRK, unpublished report). "Free" is defined as > 95 area% free surface by automated mineralogy. "Liberated" is defined as between 80 and 95 area% free surface area by automated mineralogy. "Complex" refers to ternary and higher associations.

Cu-sulfide associations	Sample 01	Sample 02	Sample 03	Sample 04	Sample 05	Sample 06	Sample 07	Sample 08
Complex	30.33	11.27	12.64	7.68	6.51	5.91	7.79	14.18
Cu-sulfides:other	0	0	0.04	0.03	0.02	0.02	0.1	0.01
Cu-sulfides:silicates:carbonates	0.47	2.01	5.87	10.81	10.25	9.6	23.22	23.9
Cu-sulfides:silicates	41.71	3.89	8.44	5.12	3.1	3.59	1.77	4.11
Cu-sulfides:carbonates	0.09	0.26	0.67	1.47	1.6	4.16	2.13	3.65
Cu-sulfides:oxides	0.37	0.34	0.19	1.22	1.37	0.97	1.86	0.21
Cu-sulfides:micas	0.96	0.03	0.24	0.07	0.03	0.01	0	0
Cu-sulfides:chlorite/clays	0.1	0.18	0.11	0.08	0.02	0.12	0.05	0.15
Cu-sulfides:feldspars	0.08	0	0	0	0	0	0	0
Cu-sulfides:quartz	0.58	5.13	10.46	10.92	8.2	5.76	3.31	4.49
Cu-sulfides:other sulfides	0.02	0.01	0	0.01	0	0	0.01	0.03
Cu-sulfides:Co-carbonates	0.04	0.23	0.07	0.02	0.04	0.01	0	0
Cu-sulfides:chrysocolla	0.16	0.24	0.2	0.06	0.08	0.24	0.16	0.31
Cu-sulfides:malachite	1.61	0.44	1.25	0.47	0.06	0.44	0.8	1.31
Cu-sulfides:native Cu	0	0	0	0.01	0	0	0	0
Cu-sulfides:carrollite	0.21	25.48	13.45	2.94	4.51	4.52	1	2.51
Liberated Cu-sulfides	5.12	15.44	13.91	11.86	15.91	16.88	12.6	12.38
Free Cu-sulfides	18.14	35.03	32.46	47.23	48.31	47.77	45.22	32.77
Totals	99.99	99.98	100	100	100.01	100	100.02	100.01
Carrollite associations								
Complex	43.17	15.09	18.12	14.94	4.65	3.38	8.37	19.38
Carrollite:other	0	0.01	0.01	0.07	0.02	0	0	0
Carrollite:silicates:carbonates	0.05	0.91	1.23	4.34	2.01	2.95	5.93	3.38
Carrollite:silicates	2.18	0.95	1.79	0.83	1.14	0.46	0.29	0.26
Carrollite:carbonates	0	0.05	0.27	1.08	1.58	3.39	1.07	0.38
Carrollite:oxides	0	0	0	0	0.03	0	0.03	0
Carrollite:micas	0.08	0.01	0.04	0.04	0.16	0	0	0
Carrollite:chlorite/clays	0.27	0.14	0.06	0.03	0.09	0.12	0.3	0
Carrollite:feldspars	0	0	0	0	0	0	0	0
Carrollite:quartz	0.6	4.16	3.4	2.07	2.01	2.07	1.05	1.27
Carrollite:other sulfides	0	0	0	0	0	0	0	0.15
Carrollite:Co-carbonates	0.76	0.08	0.26	0.24	0.08	0	0.12	0
Carrollite:chrysocolla	0.27	0	0.04	0	0.01	0	0.02	0.1
Carrollite:malachite	0	0	0	0.04	0	0	0	0
Carrollite:native Cu	0	0	0	0	0	0	0	0
Carrollite:Cu-sulfides	21.15	34.92	16.47	16.86	6.61	5.99	5.4	13.56
Liberated carrollite	11.59	20.25	24.38	17	20.24	20.29	27.86	18.64
Free carrollite	19.87	23.43	33.93	42.47	61.37	61.35	49.56	42.89
Totals	99.99	100	100	100.01	100	100	100	100.01

Freeport-McMoRan Technology Center in Tucson using established in-house protocols.

Bond index testing used 700 mL volumes of crushed, screened sample measured in a 1L graduated cylinder. This was placed in a laboratory ball mill and run for 100 revolutions at 70 rpm, with screen oversize returned to the mill and re-run until a steady state was reached.

Quick-leach testing (QLT) used 50 mL of a solution of 100 g/L H_2SO_4 and approximately 24 g/L ferric sulfate to leach 1 g sample for 1 h with agitation. Acid-soluble Cu (ASCu) was analyzed by leaching a 1-g sample in a solution of 25 mL 200 g/L H_2SO_4 plus 25 mL of 30 g/L sodium sulfite under agitation for 1 or 6 h. The same procedures and equation are used for calculating 1-hour and 6-hour ASCo.

The 2011 samples were subjected to flotation kinetic testing for both sulfide and oxide recovery. Samples of 200 g apiece were ground in a rod mill at 65 % solids with lime (CaO) dosed at the equivalent of 0.6 kg/t ore. Two minutes of conditioning at 30 % solids followed at pH 9.5, with doses of 18 g/t Cytec 10059, 18 g/t SIBX, and 20 g/t of a blend of MIBC and X-133. Standard kinetic testing was performed with a rapid flow rate of solids reporting to concentrate ("fast pull" or "high mass pull") with sampling at 45 s and 2, 8 and 24 min on three different grind sizes, with P80s of 67, 96, and 117 μm. A modified standard kinetic test was also performed at fast pull after adding NaHS to adjust ORP to approximately 70 mV vs. Ag/AgCl. These used grind sizes of 77, 92, and 117 μm but conditions were otherwise the same. Feeds and tails were analyzed by QEMSCAN and XRD for bulk mineralogy and Cu and Co deportment. The same procedure was followed for the 2012 samples, except that the charge was 1.2 kg, ground at 60 % solids, and CaO was added to attain pH of 9.5 rather than at a specific dose and 13 g/t of SIBX was added. A flowchart for flotation testing is shown in Fig. 5.

Each flotation test used only a single sample; a few duplicates were spot-tested separately. Flotation test results were tested by balancing mass and contained Cu between feed, concentrate, and tails. However, the flotation data presented below should be used with some caution as single flotation tests are often not fully balanced, and the datasets did not include residual errors or other means of checking test accuracy.

Samples from 2018 (Table 3) were shipped to Lakefield, Canada and tested by SGS Minerals (SGS, unpublished 2020 Final Report 14401). Each sample included multiple 200 L drums, of which one was selected at random. Approximately 2 kg of the coarse (>10-cm) material were randomly selected and the pieces were cut, mounted, and polished for QEMSCAN and petrographic mapping. The remainder of the drum was crushed to 1″ and blended in a drum tumbler. From this blended material, 50 kg was riffled, crushed to 100 % passing 10 mesh (2 mm), and further riffled. Each 50 kg sample yielded 4 10-kg charges for flotation testwork and 5 2-kg charges, one of which was used for chemical and mineralogical analysis. Material not used was purged with nitrogen and stored under freezing conditions. One of the 2 kg splits was further reduced to 80 % passing 212 μm and a subsample assayed, including elemental analysis, sulfur speciation by Leco, and tests for total copper and cobalt (TCo, TCu), acid-soluble copper and cobalt (ASCu, ASCo),

Table 3
Overview of the samples whose data are used in this manuscript.

Year	Sampling group name	n of samples	Type	Tests or analyses
2011	"The 88"	88	Drill core composites, 0.5 to 14 kg each: 21 from Fungurume, 32 from Kwatebala, 27 from Kavifwafwaulu (Fwaulu), 8 from Tenke	Core logging XRD, QEMSCAN, assay, ASCu, ASCo Flotation and flotation kinetic testing Additional tests on these samples in 2012
2013	"The 46"	46	41 feeds from drill core composites, which were made into 4 domain composites by formation, plus 1 master composite All from Fungurume	XRD, QEMSCAN, assay Leach testing
2018	"Lakefield"	30	Samples from test shafts, totaling 550 tonnes 8 from Fungurume, 22 from Kwatebala	XRD, QEMSCAN, assay Leach testing Flotation testing Liberation and grain size analyses

and 1-hour and 6-hour leach tests in sulfuric acid. Ten samples representing a mix of coarse and fine size fractions were made into graphite-impregnated polished epoxy mounts for QEMSCAN analysis.

3. Geotechnical characteristics

3.1. Rock Quality Designation (RQD)

RQD shows strong patterns with stratigraphy and weak patterns with depth. The RSC is the unit with the highest RQD by a wide margin (Table 4). Except near the surface, it tends to consist of > 60 % of large pieces, and the frequency distribution of RQDs is heavily skewed to the right (Fig. 6). RQDs for other units are variable but lower, probably for textural reasons. The RSC is a heavily silicified, massive dolomite but has very few laminations or other discontinuities. In contrast, the other Mines Series units contain more phyllosilicate, are strongly laminated, and only have high RQDs where dolomitic (or more rarely, silica) alteration has cemented them more than usual. The DStrat has a right-skewed, vaguely normal distribution, reflecting the general cementing role of dolomite and lack of phyllosilicate-lined discontinuities. The two units with a high proportion of shale laminations, the SDB and RSF, show flat to left-skewed RQD histograms (Fig. 6).

RQD values show a slight trend toward increasing with depth. Near-surface weathering tends to destroy dolomitic alteration and thus degrade the rocks; below the supergene leached zone, intact dolomite means the core comes out in larger pieces (Fay and Barton, 2012). Zero or low RQDs are usually relatively close to the surface, and values trend toward slightly greater RQD with depth (Fig. 7). The few low RQDs at greater depth typically relate to faults or drilling problems, based on drill core observations. However, none of the observed correlations between RQD and depth approaches statistical significance due to the number of outliers.

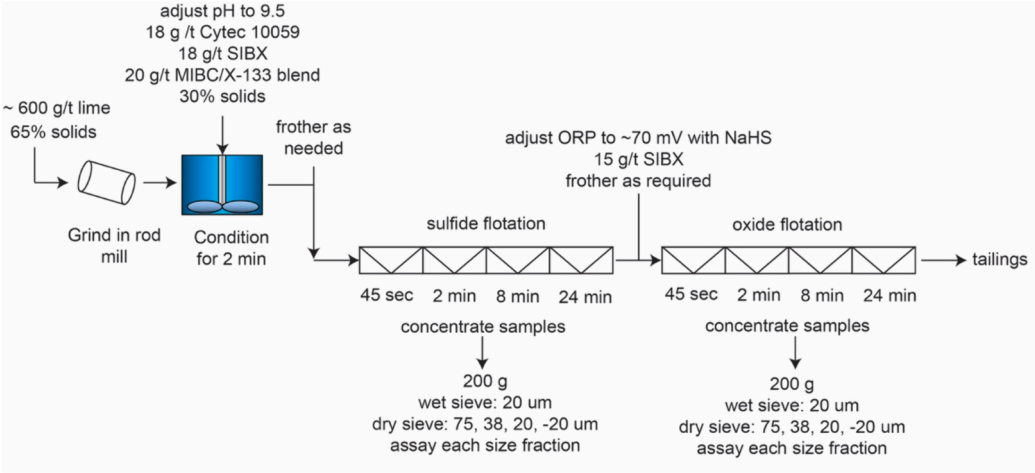

Fig. 5. Schematic of flotation testing process used to produce concentrate samples and analyses used in this study.

Table 4
Descriptive statistics of RQD and point load test results for each formation in the Mines Series.

	Point load Is50, MPa				PT gauge pressure, kN			RQD	
Unit	average ± SD	min	max	count	average ± SD	min	max	average ± SD	count
SDB	1.26 ± 1.24	0.01	10.99	2071	4.69 ± 4.45	0.03	50.69	47.19 ± 27.02	2153
RSC	4.37 ± 2.67	0.03	15.98	5621	17.04 ± 11.11	0.12	84.60	60.15 ± 28.91	5794
RSF	2.48 ± 2.21	0.05	16.16	2011	9.23 ± 8.40	0.19	63.12	50.74 ± 27.71	2069
DStrat	2.81 ± 2.24	0.04	17.55	997	10.50 ± 8.61	0.17	55.00	54.17 ± 26.32	1029

	Failure types					totals
Unit	Brittle	Mixed	Shear	Intermediate	Ductile	
SDB	1037	308	20	787	0	2152
RSC	777	1476	54	3180	0	5487
RSF	753	402	24	871	0	2050
DStrat	305	202	17	494	0	1018

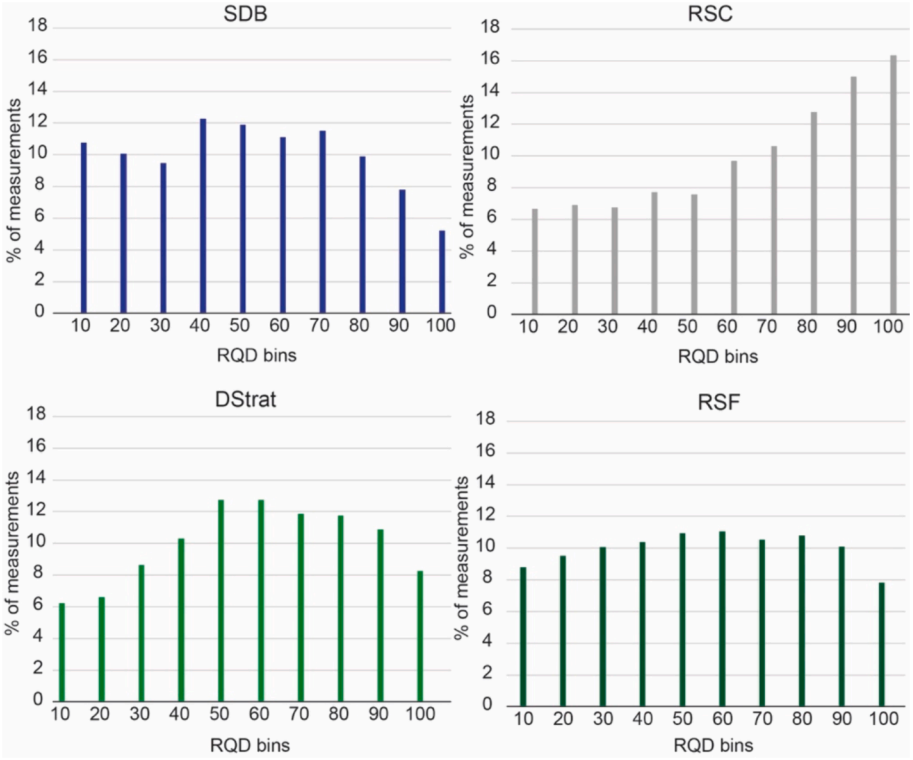

Fig. 6. Histograms showing the distribution of RQD values in Mines Series rocks at Tenke-Fungurume, based on core logging.

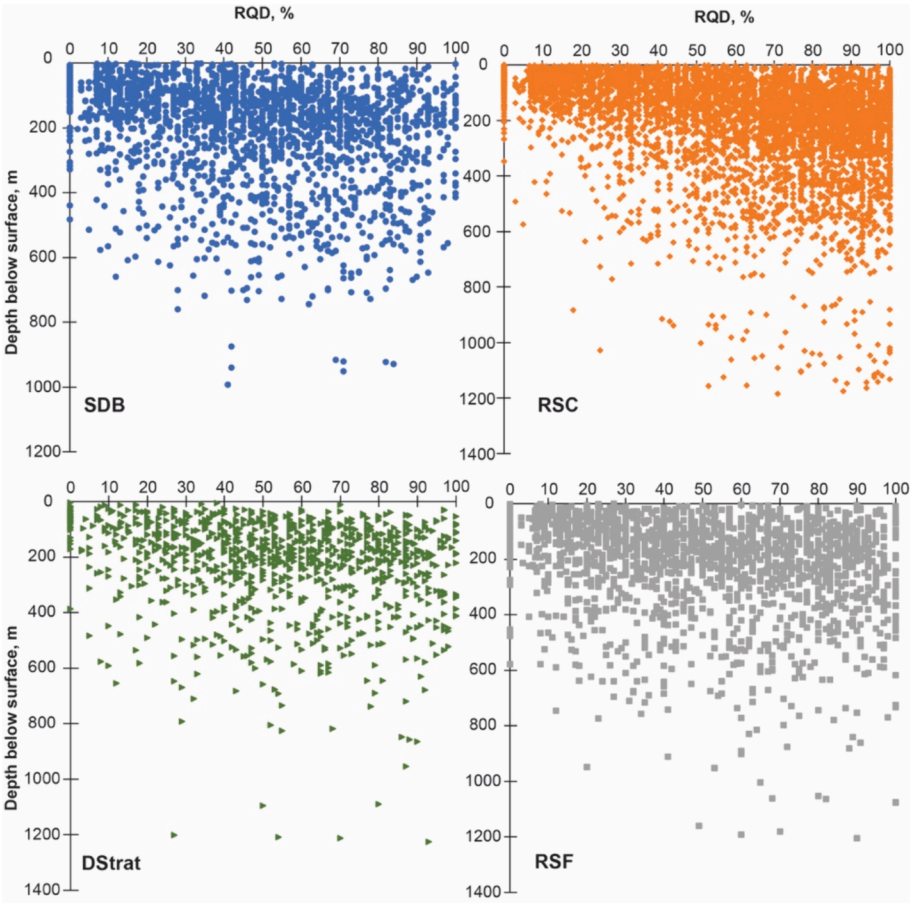

Fig. 7. Charts showing variation in RQD measurements with depth below modern topographic surface.

3.2. Point load data

Point load testing shows more scattered but similar results. The RSC stands out as the strongest unit by a factor of roughly 1.7 compared to the others and differs from them in breaking mainly by mixed and intermediate failure modes (Table 4). The other units are weaker and show a higher proportion of brittle failures. Again, the main difference is probably textural: the lack of lamination in the RSC means that it has no easy planes of breakage, whereas the others (particularly the SDB and RSF) have built-in discontinuities.

3.3. Uniaxial compressive strength (UCS)

Interestingly, the small number of UCS tests performed showed the opposite trends to point load and RQD data. Measured by UCS, the RSC is the weakest unit of the Mines Series with the narrowest strength distribution (Table 5). We assume that UCS tests on laminated rocks were performed perpendicular to the direction of any lamination in the rock. If that were the case, the difference might be explained by the abundant coarse dolomite in the RSC below the near-surface cobalt cap (Fig. 2). It typically forms large rhombohedra filling fenestrae or cavities in the rock, some of which exceed 5 cm in width. This cleaves readily under relatively low pressure. If the tested rock contains a zone or plane with all coarse dolomite and little or no silica, a high RQD and a low UCS might be expected. Conversely, applying the UCS test perpendicular to laminations in other units would negate the effect of lamination, leading to an artificially high UCS for a rock that would break easily with a slight change in orientation. However, the number of UCS data points is too small to support reliable conclusions, and we were unable to confirm the direction of UCS testing. Attempts to correlate UCS with observed mineralogical and geological features failed in all stratigraphic units.

Table 5
Statistics of the comminution characteristics for each formation in the Mines Series, including crusher work index (CWI), grinding Bond work index (BWI), uniaxial compressive strength (UCS), and abrasion index (Ai). All CWI and BWI values are in kWh/t.

Unit	CWI mean ± SD CWI min / max # of samples	BWI mean ± SD BWI min / max # of samples	UCS mean ± SD, psi # of samples	Ai mean ± SD, g/rev # of samples	Geometallurgy notes
SDS	not tested	14.2 ± 1.9 10.0 / 18.7 63	not tested	not tested	No observed correlation between comminution characteristics and QEMSCAN mineralogy
SDB	8.1 ± 3.6 5.4 / 17.9 10	13.4 ± 2.8 6.2 / 21.1 128	6249 ± 5343 10	0.046 ± 0.062 8	No observed correlation between comminution characteristics and QEMSCAN mineralogy
RSC	6.8 ± 2.4 3.5 / 10.3 7	15.0 ± 2.4 8.1 / 20.6 113	4547 ± 3885 6	0.180 ± 0.170 8	Ai correlates with % quartz ($R^2 = 0.60$). Slight (+) correlation between BWI and UCS ($R^2 = 0.34$).
RSF	8.6 ± 2.7 5.2 / 10.9 3	15.4 ± 2.7 5.1 / 20.4 157	7591 ± 4523 3	0.156 ± 0.115 14	Slight (−) correlation between BWI and chlorite content ($R^2 = 0.29$). Very slight (+) correlation between BWI and quartz content ($R^2 = 0.17$)
DStrat	8.5 ± 1.2 7.7 / 9.4 2	12.0 ± 2.6 6.7 / 16.6 32	6082 ± 5198 2	0.125 ± 0.099 2	
RAT	6.3 ± n/a 6.3 1	10.8 ± 2.4 7.2 / 15.9 26	8660 ± n/a 1	0.014 ± n/a 1	No observed correlation between comminution characteristics and QEMSCAN mineralogy

4. Process mineralogy: Comminution

4.1. Crushing

The patterns shown in comminution testing resemble those observed in UCS and are mainly opposite to the trends of the point load data. Data points are few (23) and should be used with caution but indicate that the RSC has a low crusher work index (CWI) compared to the other main ore-hosting units. The highest average crusher work indices are in the RSF and DStrat (Table 5), which is unexpected given their thinly laminated textures.

The relationship of crusher work index to UCS is obscure (Supplementary Data). In the RSC and SDB, there is no correlation above $R^2 = 0.3$, but in the RSF UCS correlates positively with CWI ($R^2 = 0.75$). In no formation are there observable correlations between CWI and discernible mineralogical factors measured by QEMSCAN, such as quartz abundance (Table 5). Chemical correlations were similarly elusive. Unfortunately, the samples subjected to comminution testing were analyzed for only a partial suite of elements not including Si, and none of the major elements measured showed any correlation with CWI.

Overall crusher work indices are slightly higher than those obtained by Starkey and Meadows (2007) on 7 composited Tenke-Fungurume ore samples. These ranged from 5.0 to 11.1 kWh/t and averaged 8.0 kWh/t for crushing.

4.2. Grinding and abrasion

Bond work indices for grinding at Tenke-Fungurume are generally in the moderate to low end of the range (Table 5). Distributions tend to show a strong left tail (Fig. 8). Unsurprisingly, Bond work indices show a strong positive quadratic correlation with the 80 % passing size of the

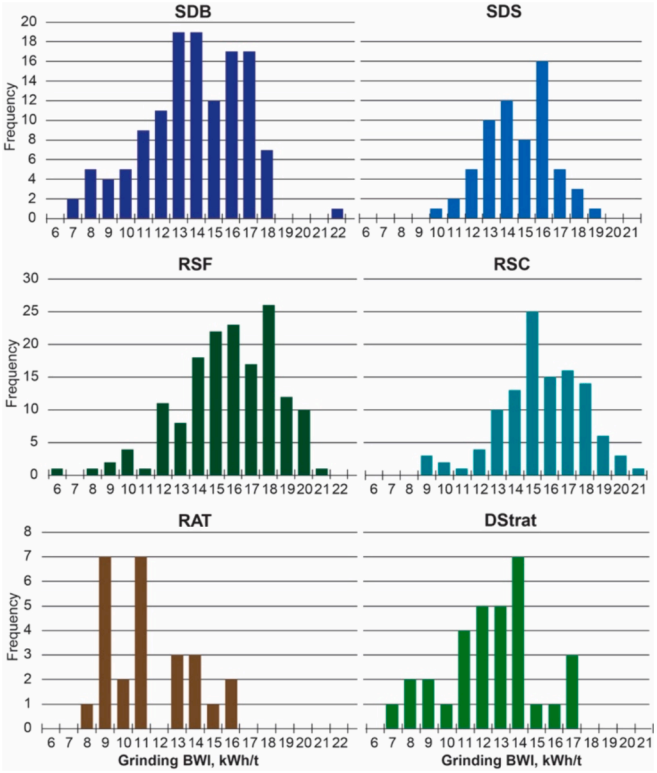

Fig. 8. Histograms of the Bond work index (kWh/t) for the Mines Series units.

ground product ($R^2 = 0.73$) and some linear positive correlation with crusher work index ($R^2 = 0.51$), particularly in the RSC and RSF ($R^2 = 0.60$ and 0.76 respectively). The same two units show a positive correlation between Bond work index and UCS ($R^2 = 0.34$ in the RSC and 0.83 in the RSF) (Supplementary Data).

High phyllosilicate content and laminated textures would be expected to make rocks more grindable (e.g. Bhuiyan et al., 2022). At TFM there is no reliable ($R^2 > 0.3$) correlation between Bond work index and phyllosilicate content, either as a group or by individual phyllosilicate type. Attempts to correlate Bond work index with other major mineral types also failed.

Abrasion indices are highest in the RSC, followed by the RSF and DStrat (Supplementary Data). Apart from these variably silicified dolomites, the rocks are generally not very abrasive. The clay-rich SDB and RAT cause almost no abrasion at all (< 0.03 g/rev), excepting a single test in the SDB with Ai = 0.178 g/rev. Only one correlation with mineralogy was observed: in the RSC, abrasion index shows a direct logarithmic correlation with quartz content (Fig. 9). In the RSF there may also be a slight trend toward increasing abrasion index with increasing quartz content, but data are too scattered to be certain. For the Mines Series as a whole, there is no significant ($R^2 > 0.3$) correlation between abrasion index and any mineral. The rocks do contain other minerals harder than steel (Mohs hardness > 5.5), such as feldspars, tourmaline, and rutile. None of these makes up more than 3–4 % of any of the rocks at most, and feldspars and rutile cleave readily and are unlikely to affect abrasion index as much as quartz. Another likely contributor to the lack of a correlation is the relatively small number of samples analyzed for both mineralogy and abrasion index.

4.3. Liberation

The grain size of intact ore varies across mineral type and rock unit. Fig. 10 shows the typical breakdown by mineralogy. Typically the gangue minerals are larger than ores, with silicates being coarsest and carbonates and Co-bearing carbonates somewhat finer. Ore grain sizes are finest, in general $d_{80} < 1$ mm, among the disseminated ores in the shale-bearing units (DStrat, RSF, and SDB); are slightly larger in dolomite veins commonly found throughout the stratigraphy; and are largest of all in the RSC.

The Cu(−Fe) sulfides are the limiting minerals for liberation (a liberated mineral is one consisting of ≥ 80 % area % of the particle). When ground, their 50 % passing particle sizes (d_{50}) ranges from slightly over 20 to a maximum of 44 μm, while for carrollite the d_{50} ranges from 18 to 97 μm equivalent spherical diameter (ESD) (SGS, 2020). In most samples, the d_{50} of the Cu(−Fe) sulfides is about half to 2/3 the d_{50} of the carrollite. At a grind size of 100 μm, 19 of 22 Kwatebala samples had > 60 % of carrollite liberated, but only one had > 60 % liberation of the Cu (−Fe) sulfides. Most samples had to be ground to nearly 50 μm to achieve 50 % liberation of the Cu minerals (SGS, 2020). Gangue associated with non-liberated grains consisted mainly of quartz and dolomite.

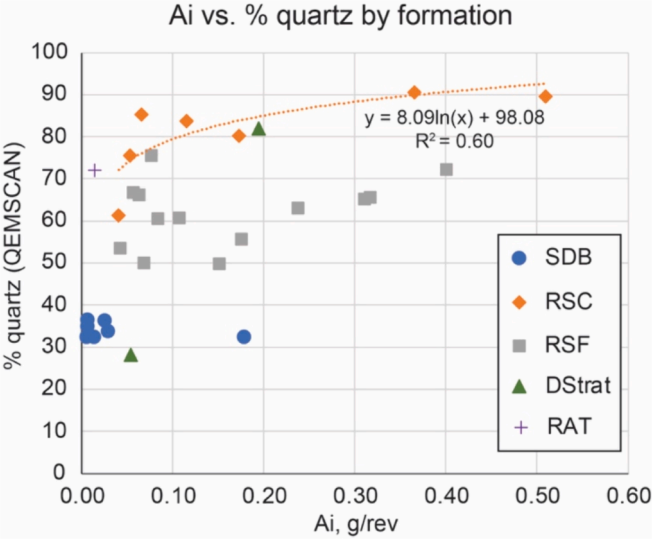

Fig. 9. Comparison between abrasion index (Ai) and amount of quartz in the sample as measured by QEMSCAN. Trendline is for the RSC only.

Liberation behavior shows significant variation with stratigraphy (Fig. 11). The lowest liberation at almost any grind size is in the SDB, unsurprising given that it hosts the ores whose grain size is both finest and closest in size to the rock-forming mineral constituents. Nodules, large dolomite veins, and other hosts of coarse-grained ore are rarer there than in the other units. At the opposite end of the spectrum, the RSF and DStrat have coarser ores, faster liberation with grinding, and higher overall liberation. The RSC is conspicuous for the steepest slopes in Fig. 11. Only three samples from the RSC were tested, but all showed the fastest increase in liberation with grinding below the coarsest fraction analyzed. This probably relates to the relatively coarse grain size of the ore compared to the grain sizes in other units.

5. Process mineralogy: Flotation

5.1. Overall recoveries by formation and mineral type

The average ultimate Cu recoveries were 87 % for the sulfide stage and 61 % for the oxide stage across all strata and a mix of oxide, sulfide, and mixed ores. Average ultimate Co recoveries were 61 % in the sulfide stage and 40 % in the oxide stage. For both metals recoveries are highest in the DStrat-RSF and lowest for the RSC and RAT (Table 6, Fig. 12). Copper recovery from the oxide stage is generally lower and more variable than for sulfides; in contrast, Co oxide recovery is lower but more consistent than for sulfides. Oxide flotation required significantly longer than sulfide flotation, with minimal recovery before the 8-minute mark.

Overall flotation recovery depends less on rock unit than on ore mineral type and, by extension, on depth below the surface. Exact rates and recoveries are difficult to pinpoint for individual minerals. However, comparative QEMSCAN analyses of feeds and tails indicates that chalcopyrite, carrollite, and bornite float extremely well, chalcocite slightly less so (Fig. 13). This is unsurprising given that chalcocite is difficult to float, requiring conditions more reducing than chalcopyrite or bornite (Lotter et al., 2016). Thus, chalcocite floated with chalcopyrite and bornite typically has lower recovery unless flotation uses a mixed collector suite. With a few exceptions, by far the largest metal losses to tailings come from the low recovery of non-sulfides. The majority of malachite, pseudomalachite, chrysocolla, heterogenite, and cobaltoan dolomite deport to tailings. Losses are particularly acute for Co in the mixed zone. Flotation recovers virtually no Co from heterogenite or cobaltoan dolomite; most Co recovered is hosted in carrollite (Fig. 13, Table 2C). A small proportion of Co is also hosted in chlorite, but its deportment to the concentrate probably does more harm than good.

With regard to depth, flotation recoveries are expected to be low among the near-surface oxides, somewhat higher in the mixed zone (particularly for Cu), and highest in the sulfide zone. This matches the results of Tijsseling et al. (2019), who estimated overall recoveries of 85 % and 75 % for sulfide Cu and Co respectively, but only 75 % and 45 % for oxide Cu and Co in Copperbelt ores.

Phyllosilicates cause most of the gangue-related problems in flotation. They begin to float almost immediately and continue to deport strongly to concentrates throughout the 24-minute testing period (Fig. 14). Their ultimate recoveries are highly variable, but are commonly > 50 % for muscovite and > 30 % for biotite and chlorite. This matches the finding by Jacobs (2016) of biotite in Kansanshi concentrates. The cause of this is uncertain, but could include entrainment or a degree of natural hydrophobicity on cleavage surfaces. It is probably

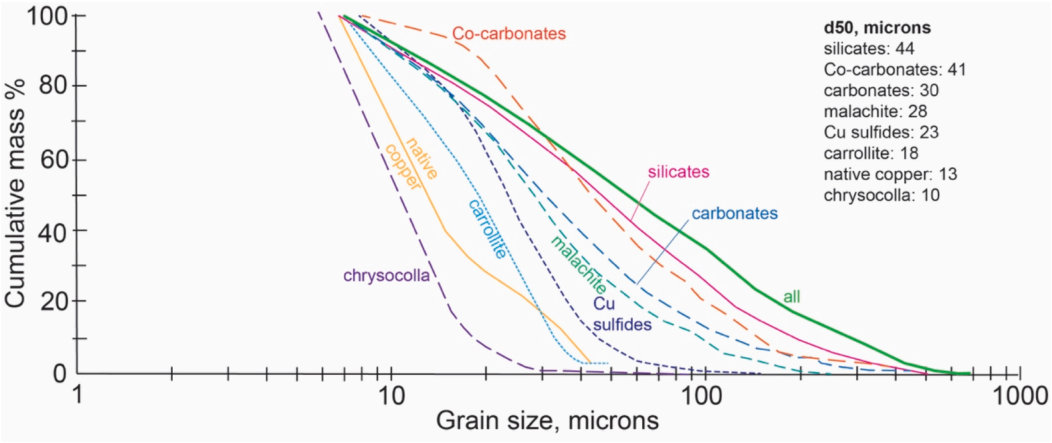

Fig. 10. Representative grain size distribution curves for the principal minerals at Tenke-Fungurume after grinding (SGS, 2020, unpub.). Sizes are shown as equivalent spherical diameter (ESD).

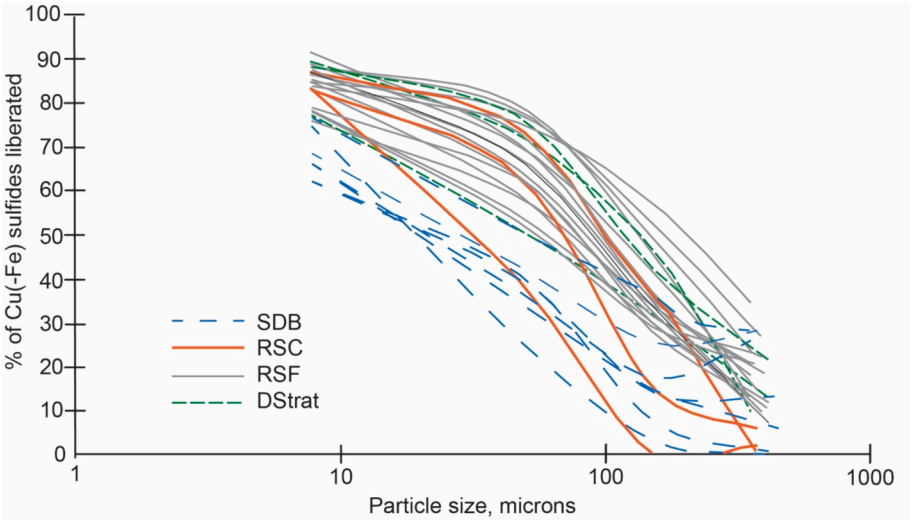

Fig. 11. Liberation curves for sulfides (chalcopyrite, carrollite, chalcocite group, bornite) based on the 2018 Lakefield samples (SGS, 2020). Sizes shown are ESD (equivalent spherical diameter).

Table 6
Flotation recoveries by formation, from the 2011 samples subjected to flotation testing (representing sulfide, oxide, and mixed ores) and 2012 re-tests. Note that ultimate recovery from oxide flotation was significantly higher than shown at the 8-minute point of comparison.

	Sulfide recovery at 8 min		Oxide recovery at 8 min	
Rock unit (n)	%Cu rec. ± SD	%Co rec. ± SD	%Cu rec. ± SD	%Co rec. ± SD
SDB (20)	84.7 ± 13.2	63.9 ± 30.2	6.8 ± 8.8	5.0 ± 4.1
RSC (21)	80.2 ± 12.4	51.6 ± 21.5	9.8 ± 9.4	6.3 ± 3.5
RSF (31)	91.4 ± 6.1	73.9 ± 24.3	2.1 ± 2.5	3.9 ± 4.1
DStrat (19)	95.0 ± 3.1	66.0 ± 25.0	1.5 ± 1.7	4.1 ± 2.5
RAT (1)	71.9 ± n/a	23.4 ± n/a	14.1 ± n/a	6.9 ± n/a

not due to phyllosilicate-sulfide composite particles, given the relatively low degree of association between them (Table 2D). Evidence from other types of ore deposits suggests that the phyllosilicates probably have a significant deleterious effect on flotation results, via sliming and excessive stabilization of froth (Forbes et al., 2017; Farrokhpay et al., 2018). This may explain the extremely low recovery from the one RAT sample tested, which averaged 12.7 % muscovite, 32.9 % biotite/chlorite, and 0.5 % undifferentiated clays by QEMSCAN – roughly twice the average phyllosilicate content of the average rock in the higher Mines Series units (Table 2A).

By contrast, less than 30 % of the quartz and dolomite in most samples ends up in concentrates, and flotation kinetics are much slower than for the phyllosilicates. There is no detectable difference in floatability between dolomite with and without Co: most dolomite ends up in tailings regardless of its metal content. While this accounts for some of the low Co recovery, dolomite is not known to cause other flotation problems.

5.2. Flotation kinetics

Fig. 15 shows representative flotation data for each ore-hosting rock formation and models derived from them. As these indicate, recovery is mainly flat after 8–10 min of flotation except for gangue, which continues to report to the concentrate through the end of the test. Notably, flotation for the master composite is slightly slower and total recovery is lower than for either the RSF-DStrat or SDB at comparable grind sizes. Flotation kinetics for Cu are relatively uniform, in contrast to the more variable rates of Co flotation in the same samples (Fig. 15). Grind size exercises a significant influence on results: coarser ores take longer to float and have lower overall recovery.

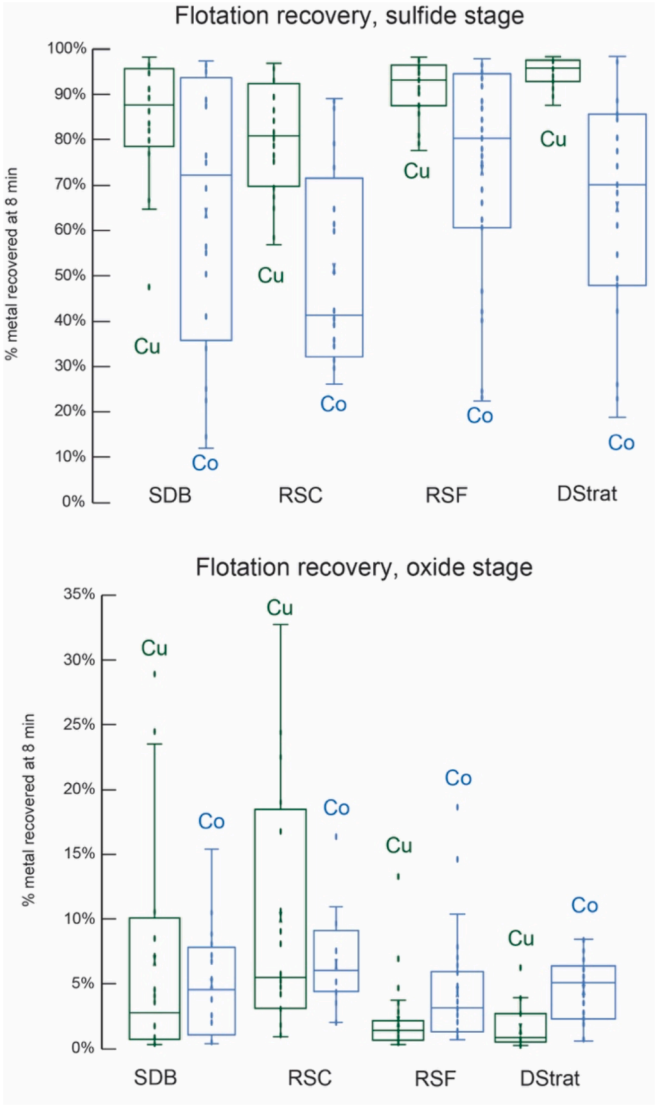

Fig. 12. Box-and-whisker plots of 24-minute flotation recovery for Cu (green) and Co (blue) by formation at TFM, based on the 2011 samples and 2012 retests. Note y-axis scale change between sulfide and oxide flotation results. (For interpretation of the references to color in this figure legend, the reader is referred to the web version of this article.)

6. Process mineralogy: Leaching

6.1. Metal recovery

Leaching in practice recovered an average of 92.5 % Cu (2009–2016 FCX Annual Reports). Cobalt recoveries were estimated for reserves, but not for production; in general, actual recovery was lower than design (R. North, unpub. data). Metallurgical testing showed, unsurprisingly, that the leachability of both metals is primarily a function of ore mineralogy with ancillary effects from rock type. The observed range of QLT %Cu and %ASCu for the Mines Series units and ore minerals are shown in Tables 7-8. (See section 2 for description of QLT and ASCu/ASCo.).

Despite the relatively clear separation between minerals' solubility ranges, connections between individual minerals and leaching test results are obscure and correlation is generally poor. It is more useful to aggregate the data by associated mineral groups, e.g. sulfides, and compare them with relevant metallurgical variables (Table 2D). As an example, the fraction of total Cu that is acid-soluble (ASCu/TCu) correlates poorly with individual sulfides, but when chalcopyrite, chalcocite, covellite, and bornite are aggregated into a group, the result shows a strong negative correlation (R^2 = 0.96) with ASCu/TCu (Fig. 16A-B). The positive correlation between ASCu/TCu and the percentage of Cu in oxides (malachite, brochantite, chrysocolla, and other Cu oxides) is nearly as good (R^2 = 0.95). The leaching behavior of Co is more scattered since a larger proportion of it occurs in minerals in the QEMSCAN "other" category (Fig. 16C-D; Tables 2B-C). Aggregating by mineral groups still improves the correlation between ASCo/TCo and Co deportment, but probably not enough for predictive use.

As is usual in deposits of Cu and other metals with multiple valence states, this means that leaching recovery will be high in the oxide or supergene zone near the surface and can be expected to decrease with depth. In the primary sulfide zone, where partially leachable chalcocite is less common than insoluble chalcopyrite, carrollite, and bornite, leaching recovery will probably be close to nil.

In all the results Co recovery is noticeably lower than Cu recovery, and correlations with mineralogy are far less evident for Co (Fig. 16). This seems counterintuitive, since the Co mineralogy of Tenke-Fungurume is much simpler and less varied than the Cu mineralogy (Tables 2B-C). Where Cu occurs in a dozen different minerals, Co is limited to heterogenite, cobaltoan dolomite, and carrollite. Some of the low leach recovery may come from insoluble components of heterogenite: mixed metal oxide or "wad" ores can be notoriously refractory to leaching depending on their composition, and this is probably just as true for cobalt wad as for copper wad. However, it is also possible that unconventional, minor ore minerals contain more Co than is generally thought. Cobalt readily substitutes for Fe in silicates and oxides, and Co in an iron-dominated oxide or a silicate lattice will be far less soluble than heterogenite or cobaltoan dolomite. Microprobe analysis of chlorites from Tenke-Fungurume has already found that they contain an average of 1.96 % Co, at least some of which consists of small domains of Co oxide (Tillotson, 2023). At an average chlorite content of 4–6 % in the main ore-hosting units and much more in the RAT, these two factors could subtract a small but non-negligible amount from Co recovery.

6.2. Acid consumption

Consumption of acid by gangue has been the single largest process expense during Tenke-Fungurume oxide leaching operations. Average acid consumption from the extensively tested 2013 samples is approximately 350 kg H_2SO_4 per metric ton ore, with some samples reaching as high as 650 kg/t. By far the most important mineral in determining acid consumption is dolomite (Fig. 17A). The influence of dolomite means that acid consumption test results also correlate tightly with %Ca. Correlations with other elements such as Mg are shaky, since Mg is also found in other non-acid-consuming minerals, mainly chlorite. The abundance of silicate minerals shows an inverse correlation with acid consumption (Fig. 17B). This is consistent with the results of a previous geometallurgical study, which found that the intensity of dolomitic alteration is the main control on gangue acid consumption (Fay and Barton, 2012). No other chemical or mineralogical parameters correlated with acid consumption to a statistically meaningful degree. As is expected from their dolomite contents, gangue acid consumption is highest in the DStrat and lowest in the SDB (Table 9).

Of the two proxies (dolomite and calcium content), %Ca is probably the more useful index for predicting acid consumption. The correlation is slightly tighter and the prediction requires only a major-element chemical assay, which in most mines is much easier to come by than a mineralogical analysis.

It is worth noting that the anti-correlation between silicates and gangue acid consumption probably holds only for vat leaching, which operates over shorter timescales than heap or dump leaching. In the latter situations, biotite, chlorite, and other mafic silicates are major acid consumers over months to years (Baum, 1999). Chlorite in particular is a major component of the gangue in nearly all units at Tenke-Fungurume (Table 2A) and would consume significant acid if the

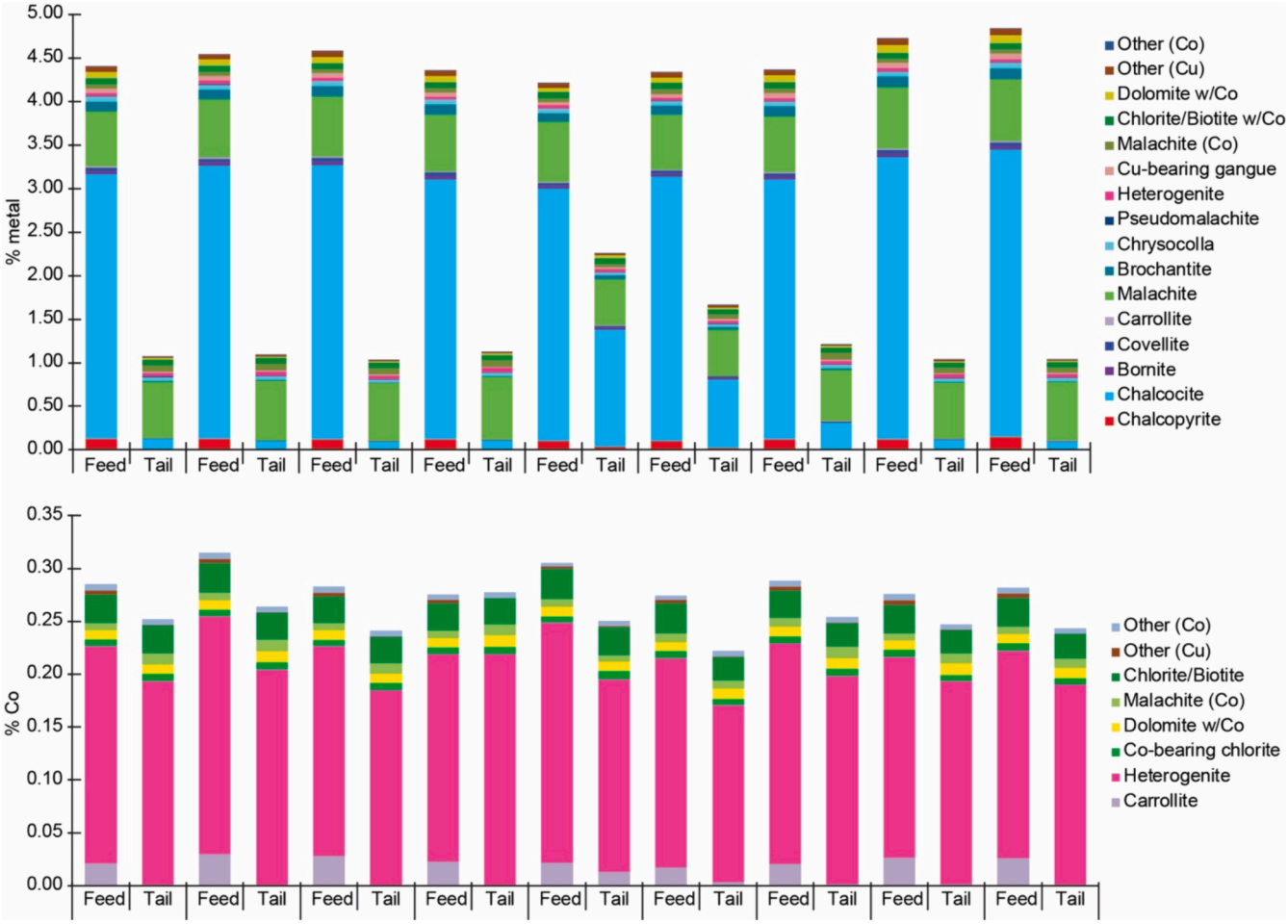

Fig. 13. Comparative feed and tail mineralogy of master composites from the 2013 samples after flotation testing. The bottom chart is from the same samples and tests as the top chart, but eliminates most Cu minerals to show Co mineralogy in more detail.

leaching process took longer. It is also likely that the chlorite dissolution would result in a silica gel, another problem for leaching (Okada et al., 2005).

6.3. Swelling clays

By comparison with gangue acid consumption, swelling clays are a minor problem for leaching at Tenke-Fungurume. Our datasets reported all swelling clays together, but a more detailed analysis indicates that nearly all of the swelling clay present at TFM is montmorillonite. The average swelling clay content in the 2012 samples, measured by XRD, is 1.7 %. While this could have a modest effect on heap leaching, it is unlikely to affect vat leaching very much compared to the impact of the dolomite.

7. Ore typing at Tenke-Fungurume

7.1. Criteria and approach

The importance of and general approach to ore typing in the mining industry is described by Barton et al. (2023). With both flotation and leaching process options available at the operation, the key ore typing questions are (1) whether the material mined contains enough metal to merit processing at all, (2) if so, which process route is better given its characteristics and the operation's economics, and (3) which data most reliably predict process outcomes and can therefore be used in assigning ore types.

Early-stage ore types at TFM are assigned based on logged mineralogy. Due to the high metal grades and high visibility of most of the ore minerals there, logging is a reasonably reliable indicator of whether grade is sufficient for mining and if so, whether the ore is oxide or sulfide. The most difficult distinction is in the mixed zone, where logging is limited to listing the three most common Cu and Co minerals each without indicating their relative abundances. This induces considerable potential for variability. For this reason, a second ore type is assigned to each interval based on metallurgical test results. If it agrees with the logging-based ore type, the case is easy; if not, a third or "best" ore type is assigned based on a ranked list of criteria. In order from highest to lowest rank, this consists of QLT, 1-hour ASCu, logged Cu mineralogy plus carrollite, and 6-hour ASCu. This is the ore type eventually modeled. The result is shown in Table 10.

While this was the method finally settled on, the original attempts at ore typing tested various different criteria for potential use in distinguishing ore types. One of these was the use of logged mineralogy as the sole criterion. This failed because while logged mineralogy is generally reliable, logging methods at the time did not record the proportions of different ore minerals, only the identities of the dominant six. This led to wide variability in metallurgical results for nominally the same ore mineralogy, rendering the logging-only method of ore typing less than useful in practice. Another attempt used the 6-hour ASCu value as one variable, but this proved unreliable since the leaching time was long enough for partial dissolution of some of the chalcocite.

This distinguishes ore typing at Tenke-Fungurume from other possible practices in Copperbelt ores. Dehaine et al. (2021) described a

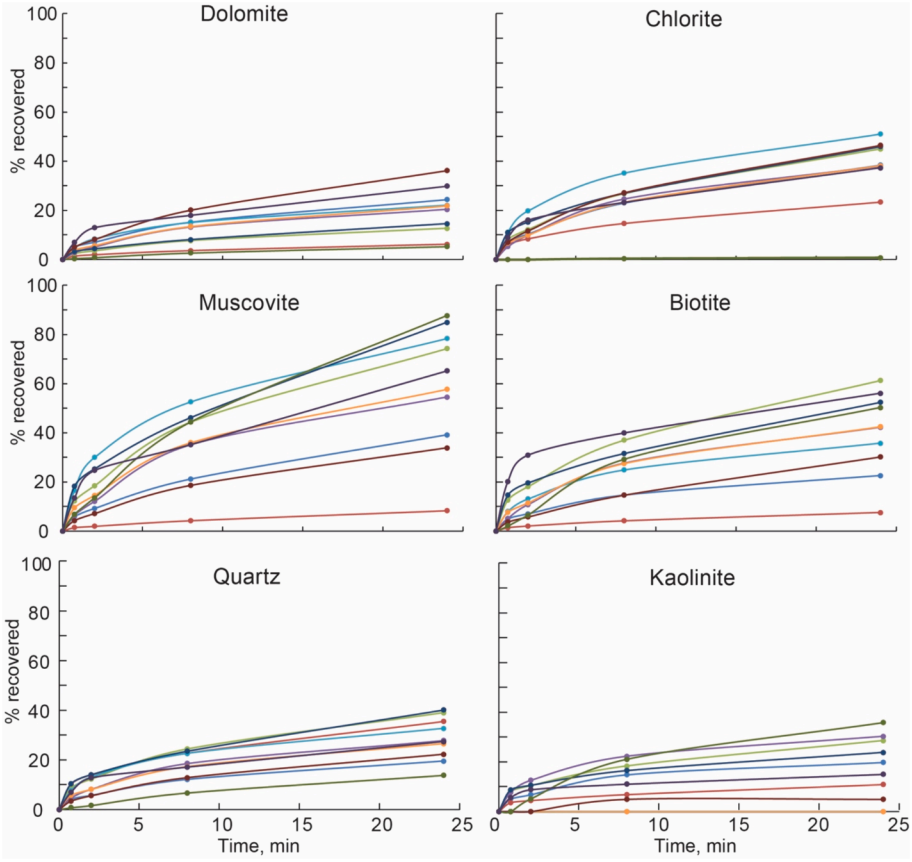

Fig. 14. Flotation kinetics of the principal gangue minerals at TFM during selected flotation tests (sulfide stage) on the 2013 samples.

method of ore typing at an unnamed deposit with similar characteristics. In that case ore types were assigned based primarily on mineralogy determined by FTIR and QEMSCAN, with ASCu and ASCo used as ancillary criteria. Otherwise, ore typing procedures for sediment-hosted Cu-Co deposits are largely unpublished.

In practice, modeling at TFM applied a series of geometallurgical domains that combined ore type (Table 10) and stratigraphic unit (Table 1). This enabled prediction of process outcomes independent of the ore types in Table 10, such as grindability. This domaining approach also provided shapes easy to model in three dimensions and retained clear connections to their geological underpinnings, making them intuitive and simple to explain by reference to geology. However, it is important to note that stratigraphy is not always a major factor in geometallurgical domaining. At Tenke-Fungurume patterns of geometallurgical behavior depend partly on stratigraphy, but in other ore deposits it may not be related to the expected process outcomes.

7.2. Spatial distribution of ore types and geological controls on process behavior

The characteristics and process behavior of each ore type vary little across the district. Minor variation in mineral compositions and proportions has been documented at various deposits or parts of deposits (Schuh et al., 2012; Santoro et al., 2019). Anecdotally, the sulfide mineral assemblage below the oxidized zone at Tenke-Fungurume may grade from chalcocite-dominated in the eastern (Fungurume) end to bornite-dominated in the central and western (Dipeta, Kwatebala) parts of the district. No type of lateral variation is known to have a significant effect on processing.

The main influences on process behavior at Tenke-Fungurume are (1) depth below the modern land surface and (2) the lithology of the rock hosting the ores. Depth is the first-order control on geotechnical properties, grade (to an extent), and overall ore type in Table 10. The "leached" ore type is exclusively found within < 50 m from the surface while primary sulfides are entirely at depths > 100 m, more often > 200 m (schematic in Fig. 18). Oxidation extends to its greatest depths along fluid-channeling faults and relatively permeable units such as the RSC. Depth below surface also determines recoveries from leaching and flotation. Leaching recovery is high in the oxide zone, then decreases with depth to a very low level in the primary sulfides. Conversely, flotation recovery is very high in the sulfide zone but mediocre among the oxides, with the mixed zone between the two having the lowest recovery of all. These mineralogy-metallurgy correlations are tight but obvious and, in a sense, trivial. The trend from leached to supergene oxides down to sulfides, and attendant changes in recovery, have long been established across multiple types of copper deposits (Anderson, 1955).

At a less obvious, second-order level, the lithology of the host rock controls the grade and the precise characteristics of the sulfide, oxide, or mixed ore present. In the oxide zone the influence of lithology is relatively low except for its effect on gangue acid consumption (Table 9; Fay and Barton, 2012). In the sulfide zone, ore grain size, liberation size, grindability, and abrasion index all depend on lithology. Fig. 19 summarizes the relationship between rock type and comminution, flotation, and leaching behavior.

Comminution work indices and a few other metallurgical variables show little obvious connection to depth, host rock type, or any other geological parameter available. This is surprising, since basic process mineralogy considerations indicate that mineralogy should have a strong and straightforward effect on comminution outcomes, at least in some respects (e.g. Gent et al., 2012). There are two likely reasons for the lack of a correlation and they are not mutually exclusive. One is that the relative abundance of different hard and non-cleaving minerals matters less to comminution than their grain size and the overall texture

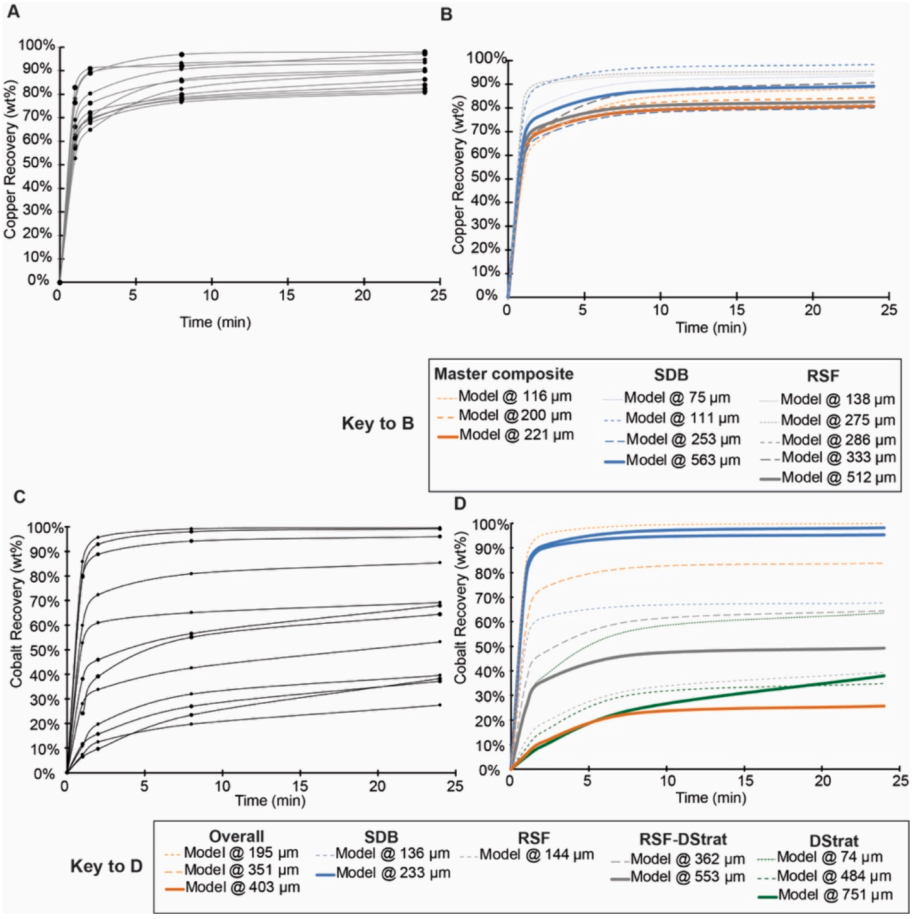

Fig. 15. Standard kinetic test results and models showing cumulative Cu and Co recovery in the sulfide stage of the rougher flotation circuit (2011 samples and 2012 re-tests). A: Representative data from individual flotation tests for copper. B: Models derived from the flotation test data by regression, showing expected copper flotation kinetics for the RSF (includes DStrat), SDB, and a master composite, at different grind sizes. C: Representative data from individual flotation tests for cobalt. D: Models derived from the flotation test data, showing expected flotation kinetics for the RSF, DStrat, combined RSF-DStrat, SDB, and the overall model, at different grind sizes. (There are two tests for the SDB at 233 µm in D.)

Table 7
Average grades and acid solubility of ores, ± one standard deviation, from each formation. Data are from the 2011 samples representing oxide, sulfide, and mixed ore types.

Rock unit (n)	% Cu	% Co	% QLT Cu	1-hour % ASCu	6-hour % ASCu	1-hour % ASCo	6-hour % ASCo
SDB (17)	3.70 ± 2.49	0.50 ± 0.46	1.77 ± 1.31	0.59 ± 0.59	1.62 ± 1.05	0.12 ± 0.19	0.15 ± 0.23
RSC (20)	2.33 ± 1.96	0.52 ± 0.50	1.27 ± 1.10	0.59 ± 0.59	1.26 ± 0.91	0.18 ± 0.22	0.25 ± 0.33
RSF (25)	4.54 ± 1.65	0.24 ± 0.26	1.79 ± 1.06	0.31 ± 0.47	1.84 ± 0.99	0.03 ± 0.04	0.03 ± 0.05
DStrat (16)	4.04 ± 2.47	0.13 ± 0.20	1.64 ± 1.10	0.32 ± 0.35	1.77 ± 1.12	0.02 ± 0.02	0.02 ± 0.03
RAT (1)	1.8 ± n/a	0.06 ± n/a	1.04 ± n/a	0.57 ± n/a	1.13 ± n/a	0.02 ± n/a	0.04 ± n/a

Table 8
Leach test recovery from pure separates of Cu minerals common at Tenke-Fungurume. Approximated after unpublished 2015 internal FMI report and confirmed on actual results from subsequent tests on TFM material with QLT and ASCu analyses as well as detailed mineralogy by QEMSCAN and/or XRD.

Mineral	% QLT Cu	1-hour %ASCu
Malachite	> 90 %	> 90 %
Chrysocolla	> 80 %	> 80 %
Pseudomalachite	> 90 %	> 90 %
Native Cu	50 %	< 5 %
Chalcocite	50 %	< 20 %
Bornite	30 %	< 5 %
Chalcopyrite	< 10 %	< 10 %

in which they are arranged into the rock. Even extremely hard minerals are easy to crush and grind if the rock is thinly laminated and the minerals are already fine in grain size. The second source of confusion arises from the nature of crushing and grinding tests. Comminution work index tests are notoriously difficult to perform and outcomes vary greatly with the skill and experience levels of the operator (Mwanga et al., 2015). Unless all the tests were performed by the same technical team under the same conditions at similar times, the results may not be fully comparable. Tentatively, both of these factors may be at work in the present comminution dataset. The use of large composited samples is a potential additional source of variability, but in this dataset was minimized by compositing only within units and supporting the composite tests with samples exclusive to individual units.

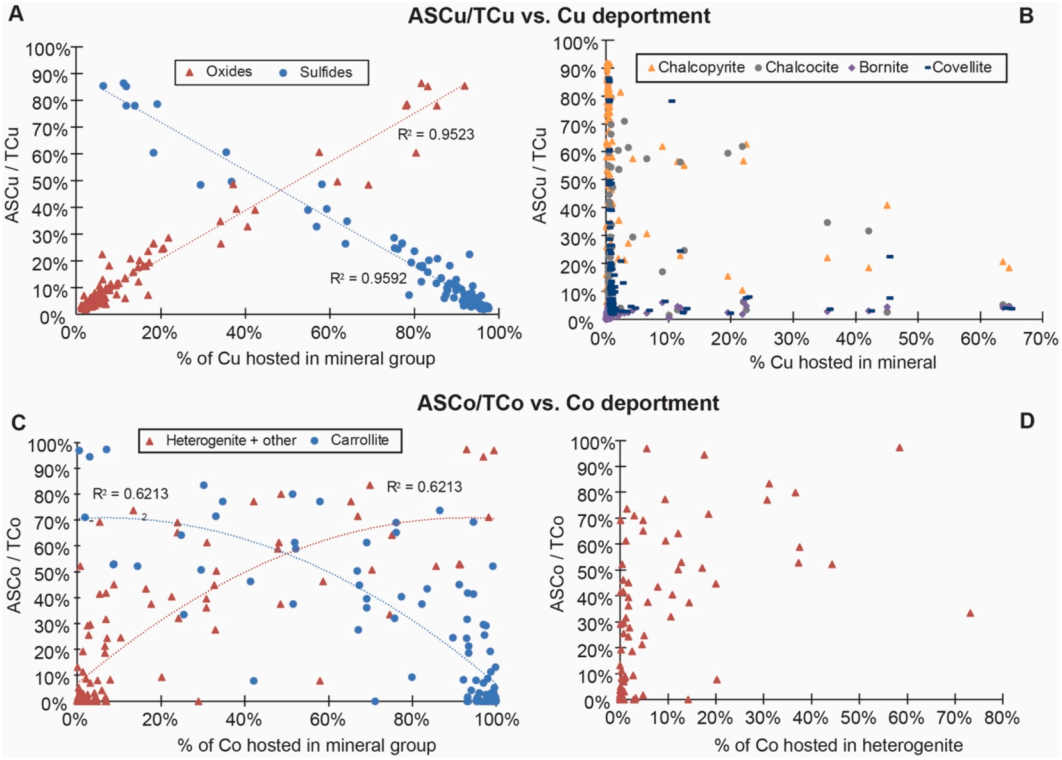

Fig. 16. The relationship of soluble metal to mineral deportment is clear when ore minerals are aggregated into groups (A,C), but is obscure when considering minerals individually (B,D).

Table 9
Average acid consumption test results and related parameters for each formation in the Mines Series at Tenke-Fungurume and overall, based on 4 domain composites of individual formations and 1 master composite of ores from all formations (2012 tests).

Formation	Calculated acid consumption, kg H_2SO_4 / metric ton	% carbonate	% Ca	%Si
SDB	226.2	14.1	3.9	23.3
RSC	351.8	18.4	6.4	25.6
RSF	350.9	20.3	6.4	25.1
DStrat and RAT	435.1	26.6	8.1	17.8
Master composite	345.1	20.7	6.2	23.5

8. Discussion

8.1. *Effects of Copperbelt mineralogy on processing*

Existing literature on the process mineralogy of Copperbelt deposits is thin, and mainly focused on lab-scale analyses of the process behavior of particular mineral types. The analyses of this production-scale dataset show varying levels of correspondence with previous lab-scale conclusions.

8.1.1. *Ore minerals, supergene to mixed*

Extraction from most ore minerals at Tenke-Fungurume is relatively straightforward on an individual basis. The main problem in extraction arises from mixed ores, since very few metallurgical processes can recover Cu and Co from both sulfides and oxides. This is a longstanding problem for Cu (e.g. Hanson and Fuerstenau, 1991; Lee et al., 2009), but worse for Co. The combined leach-roast operation at Luilu is one of the only operations that recovers most Co from both oxide and sulfide ores

Table 10
Ore types used in modeling the Tenke-Fungurume district, with analytical and geological criteria used in the division. Note that in practice, modeling worked better for most deposits when the oxide- and sulfide-dominant mixed ores were combined into a single mixed zone (R. North, unpub. data).

Ore type	TCu %	QLT %	1-hr ASCu %	Logged ore mineralogy	Description; process route
Sterile	< 0.08	TCu too low for these to be meaningful		Trace pyrite / Fe oxides or none	Low grade, typically outside of Mines Series; not processed
Leached	< 1.0	30 – 62.5	25 – 60	Fe oxides plus Co oxides that may remain.	Ores removed by supergene alteration; commonly minor grade but too low to process
Oxide	> 0.10	75–100	70–100	Malachite, heterogenite, chrysocolla	May be subdivided into high- and low-acid-consuming types; leach
Oxide-dominant mixed	< 15.0	62.5 – 95	35 – 70	Oxides plus chalcocite and cobaltoan dolomite	Used when chalcocite is a significant component of otherwise oxide ores; leach
Sulfide-dominant mixed	0.2 – 15.0	52 – 70	2.5 – 35	Sulfides plus malachite and cobaltoan dolomite	Mainly chalcocite with accessory chalcopyrite and malachite; float
Sulfide	0.2 – 15.0	0 – 52	0 – 2.5	Chalcopyrite, bornite, carrollite, chalcocite	Primarily chalcopyrite-carrollite and other sulfides with almost no oxide; float

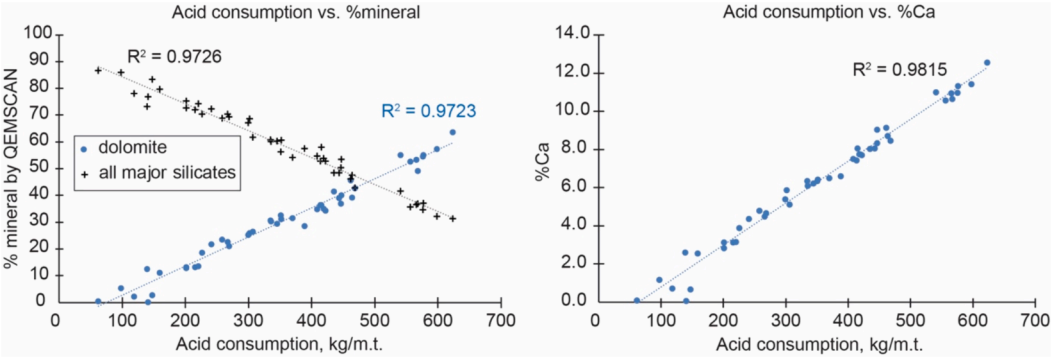

Fig. 17. Acid consumption is controlled by mineralogy, particularly the abundances of acid-neutralizing dolomite and acid-stable silicates (left, A). Calcium content in the rock makes a good proxy for acid consumption (right, B).

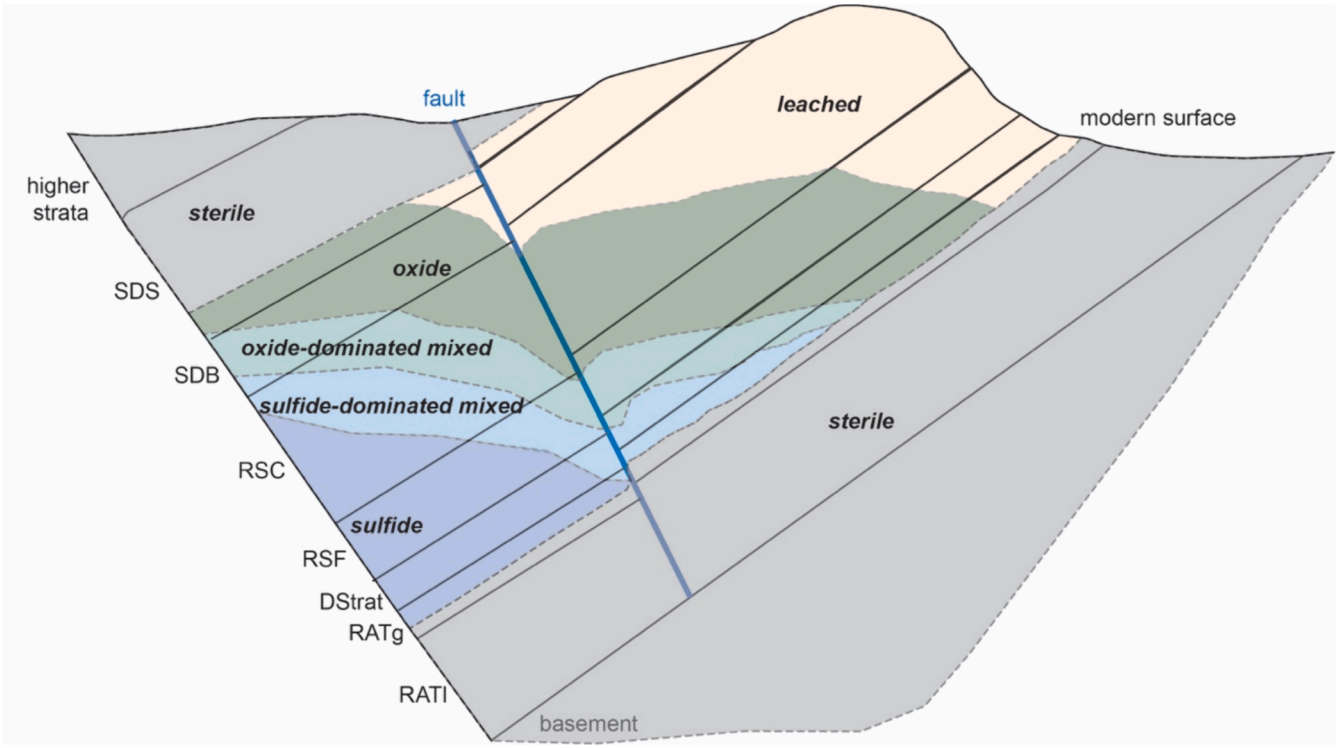

Fig. 18. Schematic cross-section of a typical écaille at Tenke-Fungurume, showing the usual distribution of the ore types in Table 10. Not to scale. Cf. the depth profile in Fig. 2.

(Crundwell et al., 2020). At Tenke-Fungurume, flotation recovers Co from sulfides but less than half of the oxides, whereas leaching recovers > 80 % of Co from oxides and almost none from sulfides. Since Co oxides and sulfides occur together throughout much of any deposit's depth profile (Figs. 2, 18), process losses are inevitable.

Of individual ore minerals, only heterogenite, cobaltoan dolomite, and native Cu are known to involve significant recovery problems. In the case of heterogenite, Santoro et al. (2019) attributed the lower Co leach recovery (compared to Cu recovery) across the Copperbelt to some fine-grained heterogenite being locked in insoluble clays and to some of the Co oxides consisting of asbolane, lithiophorite, and other Mn-rich species less soluble than heterogenite. Tillotson (2023) also found evidence of heterogenite locking by clays, but identified the insoluble Co-hosting minerals at Tenke-Fungurume as mainly cobalt-bearing chlorites rather than oxides. This study lacks most of the mineralogical specificity of those works, but the scattered recovery from heterogenite and "Co-Other" phases (Fig. 16) is consistent with their results. Cobaltoan dolomite leaches easily but is rejected along with regular dolomite in flotation. Native Cu yields poor recovery to both leaching and flotation, including in the Cu mine at Kansanshi (Little et al., 2018).

Where abundant, the incongruent dissolution of chrysocolla can lead to colloidal silica buildup in leaching circuits. Precipitates from this clog pipes and can form silica gels on anodes, a significant process issue at Luita (Alexander et al., 2018). Chrysocolla tends to be a minor to accessory phase in most of the Tenke-Fungurume ores, and this problem has not been noted in the literature or reports on the district. However, silica gels can also form from the unwanted dissolution of chlorite and other common gangue minerals in leaching, so this may not be an ore-related problem (e.g. Queneau and Berthold, 1986). The datasets in this study do not offer any grounds for definitive statements about whether silica gels form in Tenke-Fungurume leaching, from what minerals if so, and what their effects are.

8.1.2. *Ore minerals, hypogene*

The hypogene ores at Tenke-Fungurume are quite tractable to flotation. Comparisons of heads and tails show that the large majority of

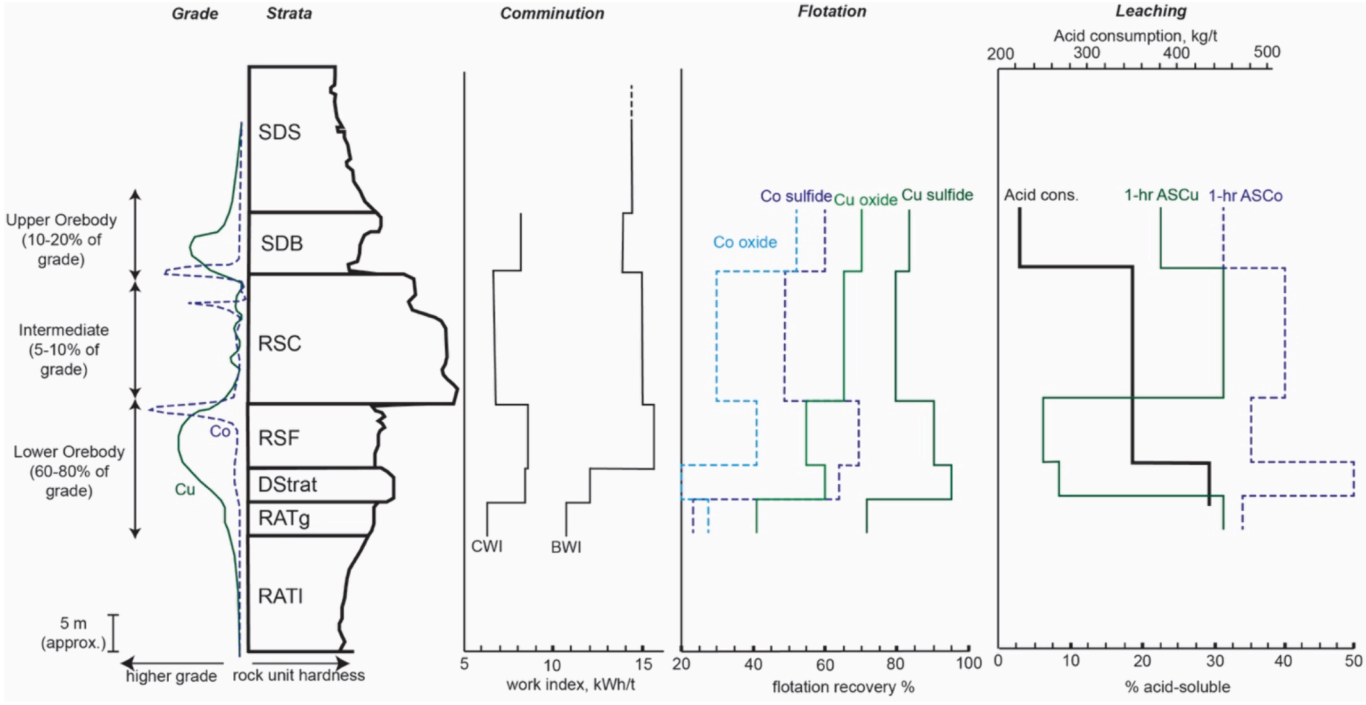

Fig. 19. Summary of variation in comminution and leaching characteristics by lithology. Grades and hardness are schematic. Comminution, flotation, and leaching values are averages for each stratigraphic domain, a.k.a. formation. See Tables 6-9 and text for more detail.

carrollite, chalcopyrite, and bornite deport strongly to concentrate. The main Cu sulfides in tailings are chalcocite and covellite. Most Cu losses in flotation of hypogene ores arise from small amounts of malachite and other supergene minerals still present (Fig. 13). This is comparable to the flotation behavior observed in other Cu deposits, where sulfides are easily recovered but oxides and related supergene minerals are lost to tailings.

Most of our flotation results are also similar to those obtained in other flotation studies on Copperbelt ores. At the Co-poor Kansanshi Cu mine in Zambia, Jacobs (2016) obtained Cu flotation recoveries of 87–90 % with lab flotation of ores consisting almost entirely of well-liberated chalcopyrite. This is consistent with the results of Little et al. (2018) from plant-scale data at the same mine, which showed high and consistent recoveries for sulfides in the hypogene zone but lower and more variable recoveries in mixed and oxide ores, attributed to more variable mineralogy. With ores from an unspecified Cu-Co mine in the Copperbelt, Tijsseling et al. (2020) obtained maximum recoveries of 74.4 % for Co and 89.8 % for Cu in a series of 7-minute flotation tests. The authors did not analyze mineralogical factors in Cu recovery, but applied a regression analysis to identify factors affecting Co recovery. They found that chalcocite content and the presence of carrollite particles > 100 μm in size both had a significant negative influence on recovery, while association with dolomite and Mg-chlorite had a positive effect (Tijsseling et al., 2020). This is consistent with our findings on flotation recovery at different grain sizes (Fig. 15). However, we found no noticeable effect from either chalcocite or dolomite being present in the feed, and chlorite appeared more likely to decrease flotation recovery than promote it. As Tijsseling et al. (2020) suggested, their finding apparent positive influence of chlorite may in fact reflect a correlation rather than a causative relationship, or perhaps the small number of samples in the study. Dehaine et al. (2021) identified a high sensitivity to pH as a potential issue. We are unable to compare our results since all flotation tests in our database took place at roughly the same pH range (~9.5).

8.1.3. *Gangue minerals*

Of the common gangue mineral types at Tenke-Fungurume (quartz, dolomite, phyllosilicates), each is responsible for a different type of problem. Quartz is inert in leaching and easily rejected in flotation, but Dehaine et al. (2021) suggested it causes moderate problems in comminution. The high hardness of quartz (7 on the Mohs scale, compared to about 5.5 for steel grinding media) and its lack of cleavage, as well as previous studies on lab-scale grinding of hard and non-cleaving minerals (Gent et al., 2012), suggest that quartz-rich rocks should have a higher grinding work index at least. The test data in the present study fail to support this. The RSC is the only rock formation in which quartz abundance shows even a hint of correlation with comminution properties, in that case abrasion rather than work index (Fig. 9). This is probably because the RSC is the formation with the fewest laminations, phyllosilicates, and other features that complicate comminution geometallurgy.

Dolomite is a large and obvious problem for leaching, where it raises acid consumption to levels that would be prohibitive for a lower-grade operation (Table 9). The test data here show that it causes no evident problems for flotation, and we found no evidence that it can have a negative effect on comminution as sometimes suggested (Dehaine et al., 2021).

In contrast, phyllosilicate minerals create problems throughout the process chain at most mines (Graefe et al., 2017), and Tenke-Fungurume has its share of these issues. There is no evidence for effects on comminution, but chlorite, muscovite, and biotite appear to be quite deleterious in flotation. Recovery is rapid and often exceeds 20 % of the phyllosilicates by 8 min (Figs. 13-14). This is consistent with Jacobs' (2016) discovery of chlorite and biotite in flotation concentrates from Kansanshi. Chlorite and biotite have also been identified as potential acid consumers in leaching, both in Copperbelt mines and in general (Baum, 1999; Dehaine et al., 2021), but this does not appear to be the case at Tenke-Fungurume (Fig. 17). This is probably because of time-scale. Though acid consumption by chlorite and biotite has been documented in long-term (months to years) heap leaching, agitated leaching puts the ores in contact with acid for 8 h or less and dissolution appears

to be minimal over that interval (Baum, 1999). At Tenke-Fungurume dolomite is practically the sole cause of acid consumption by gangue minerals (Fig. 17).

Talc has been identified as another problem phyllosilicate in Copperbelt deposits (Macfarlane and Williams, 2014), but is not present at TFM to any significant extent. We know of no reports of talc, carbonaceous material, or other hydrophobic species causing significant flotation or other processing problems at TFM.

8.2. Geometallurgy at the production scale

This research identified several significant correlations between mineralogy and metallurgy: the dependence of acid consumption on %Ca and dolomite concentration; the relationship of sulfide abundance to flotation recovery; and the influence of malachite abundance on Cu leaching recovery. These correlations are strong and clear. They are also exactly what any competent metallurgist or mineralogist would predict before seeing a single test result.

Subtler geometallurgical insights would be more important, but are obscure. For instance, the Bond work index is certainly related to the average hardness and cleavage of the minerals in a rock (Gent et al., 2012), but in our dataset there is no apparent correlation between grindability and the abundance of hard or soft minerals (Table 5 and Supplementary Data). This illustrates the need for geometallurgical measurement of factors beyond simple modal mineralogy and chemical composition. Our dataset did not include average aspect ratios of grains, lamination thickness, frequency of different mineral associations, or other quantitative textural information. Measuring these would probably enable more diverse and robust geometallurgical correlations, particularly in comminution and flotation (Tungpalan et al., 2015).

However, there are a few clear takeaways from our study. One is the danger of being too specific when trying to link geology to metallurgy at scales above laboratory work. As an example, Fig. 16 shows that overall leach test results fail to correlate with mineralogy at the level of individual sulfide minerals, but an excellent correlation ($R^2 > 0.95$) emerges when the sulfides are lumped together in one group. This probably corresponds to the ubiquitous association of different sulfide minerals with each other (Table 2D). Similarly, acid consumption correlates better with silicates as a group than individually (Fig. 17). Fine detail is always tempting, especially to academics, but in this case actually makes geometallurgy less useful.

Lastly, the analyses in this case study show the need for a genuinely interdisciplinary approach to geometallurgy. The relationship of geological inputs to metallurgical outcomes is so tangled that an approach that does not include geology, mineralogy, and metallurgy is bound to fail. With a good mix of both, failure is still possible but less likely. Geologists will better understand how the mineral and chemical features they observe impact processing (or don't), while metallurgists will operate with an appropriate respect for the complexity of the geological material they have to work with.

9. Conclusions

Process characteristics of Tenke-Fungurume Cu-Co ores depend first on depth below surface and second on host rock lithology. Depth below surface determines whether the ore is sulfide, oxide, or mixed; host rock influences the leaching and some comminution characteristics of the ore.

In comminution, there are very few correlations between geological features and metallurgical behavior. Many of the geotechnical and mineralogical features expected, in theory, to be important – such as point load index, RQD, phyllosilicate content, laminated textures, and prevalence of hard and non-cleaving minerals – do not have discernible correlations with comminution results at the production scale. The exceptions are a moderate positive correlation between abrasion index and quartz content in the one un-laminated rock unit, the RSC, and stronger positive correlations between UCS and Bond crushing and grinding work indices in the RSF. Liberation is generally limited by Cu-Fe sulfides, which are half the average grain size of the carrollite for an equivalent amount of grinding, and must be ground to roughly 50 μm to achieve 50 % liberation. There is a moderate correlation between crushing and grinding work indices.

Flotation behavior depends first on mineral type and second on rock unit. Most sulfides float with high overall recoveries. The exception is chalcocite and covellite, which are the main sulfides found in tailings. Otherwise, metal losses to tailings generally correspond to heterogenite, chrysocolla, or malachite in the feed. These show poor recovery (< 10 %) even in oxide flotation tests and are completely rejected in sulfide flotation. The main flotation problems related to gangue are muscovite, chlorite, and biotite, which deport to the concentrate and reduce recovery, perhaps by sliming. Dolomite, cobaltoan or otherwise, deports to the tailings along with quartz. Average final (24-minute) recoveries across all units and ore types are 87 % for Cu sulfides, 61 % for Co sulfides, 61 % for Cu oxides, and 40 % for Co oxides.

Leaching recovery shows a strong inverse correlation with sulfide abundance and a strong positive correlation with oxide abundance, but only at the group level. Correlations weaken and disappear at more granular levels, such as considering recovery as a function of individual sulfide type. The main leaching expense is sulfuric acid, as gangue acid consumption averages 345 kg acid per metric ton ore. Gangue acid consumption correlates strongly with %Ca and dolomite abundance and is unrelated to the contents of chlorite, biotite, and other long-term acid consumers, probably due to the short timescales of vat leaching. Other leaching problems such as silica gel generation and losses due to swelling clays are not reported at Tenke-Fungurume.

These process behaviors determine the six ore types at Tenke-Fungurume: sterile, leached, oxide, sulfide, and two mixed types dominated by oxides and sulfides respectively. Criteria used in ore typing are primarily leach test results and logged ore mineralogy. Ore type distribution patterns depend first on depth and second on rock formation. Near the surface, all formations are either sterile or leached. Going downward, the rocks zone through oxide, oxide-dominated mixed, sulfide-dominated mixed, and sulfide ores. These are combined with stratigraphic units to yield the modeled geometallurgical domains.

The results of this study also demonstrate the challenges of operational geometallurgy. Most of the mineralogy-metallurgy correlations that are strong enough for prediction are also generally trivial: dolomite and %Ca correlate with gangue acid consumption, for instance. More complex and useful geometallurgical relationships, such as the effects on flotation of specific minerals or the prediction of comminution behavior, are more obscure. This illustrates the need for geometallurgy to include not only modal mineralogy and chemical composition, but other factors such as rock texture and fabric that are less frequently quantified.

CRediT authorship contribution statement

Isabel F. Barton: Writing – review & editing, Writing – original draft, Project administration, Methodology, Investigation, Formal analysis, Conceptualization. **Robert M. North:** Writing – review & editing, Writing – original draft, Resources, Methodology, Investigation, Formal analysis, Data curation.

Declaration of competing interest

The authors declare the following financial interests/personal relationships which may be considered as potential competing interests: [Isabel Barton reports financial support was provided by National Science Foundation. Both authors were previously employed by Freeport-McMoRan Inc. (Barton, North). Co-author was previously employed by CMOC (North). If there are other authors, they declare that they have no known competing financial interests or personal relationships that could have appeared to influence the work reported in this paper].

Data availability

Data will be made available on request.

Acknowledgments

The metallurgical and geological datasets used as the basis for this paper were accumulated over several years by Freeport-McMoRan Inc. and consulting companies working for them. Insights made over this time by Sebastian Lavoie, Jodie Robertson, and many others were particularly valuable in developing the methods and conclusions presented here. We thank Freeport-McMoRan Inc. and CMOC for permission to publish this work. Suggestions from two anonymous reviewers greatly improved the manuscript.

The new analyses presented in this work, and the writing and drafting, were supported by NSF grant #20-45277 to I. Barton.

Appendix A. Supplementary material

Supplementary data to this article can be found online at https://doi.org/10.1016/j.mineng.2024.108993.

References

Alexander, D., Van der Merwe, C., Lumbule, R., Kgomo, J., 2018. Innovative process design for copper-cobalt oxide ores in the Democratic Republic of Congo. J. South Afr. Inst. Min. Metall. 118, 1163–1170.

Anderson, C.A., 1955. Oxidation of copper sulfides and secondary sulfide enrichment. Economic Geology 50th Anniversary Volume 324–340.

Bartholomé, P., Evrard, P., Kateesha, F., Lopez-Ruiz, J., Ngongo, M., 1973. Diagenetic ore-forming processes at Kamoto, Katanga, Republic of the Congo. In: Armstutz, G. C., Bernard, A.J. (Eds.), Ores in Sediments. Springer-Verlag, Heidelberg, pp. 21–41.

Barton, I.F., Yang, H., Barton, M.D., 2014. The mineralogy, geochemistry, and metallurgy of cobalt in the rhombohedral carbonates. Canadian Mineral. 52 (4), 653–670.

Barton, I.F., Robertson, J.M., Caro, C., 2023. Ore types: what they are, how they're made, and their uses and abuses. Mining, Metallurgy, & Exploration 40, 2153–2160.

Baum, W. (1999). The use of a mineralogical data base for production forecasting and troubleshooting in copper leach operations: Copper 99, Proceedings, v. IV, Miner., Metals Mater. Soc., 393-408.

Bhuiyan, M., Esmaeili, K., Ordonez-Calderon, J.C., 2022. Evaluation of rock characterization tests as geometallurgical predictors of bond work index at the Tasiast mine Mauritania. Minerals Eng. 175, 107293.

Boisvert, J.B., Rossi, M.E., Ehrig, K., Deutsch, C.V., 2013. Geometallurgical modeling at Olympic Dam mine, South Australia. Math. Geosci. 45, 901–925.

Cailteux, J., 1994. Lithostratigraphy of the Neoproterozoic Shaba-type (Zaire) Roan Supergroup and metallogenesis of associated stratiform mineralization. J. African Earth Sci. 19 (4), 279–301.

Coward, S., Vann, J., Dunham, S., and Stewart, M., (2009) The primary-response framework for geometallurgical variables. Proceedings of the 7th International Mining Geology Conference 109-113.

Crundwell, F., Du Preez, N.B., Knights, B.D.H., 2020. Production of cobalt from copper-cobalt ores on the African Copperbelt – an overview. Miner. Eng. 156, 106450.

Dehaine, Q., Tijsseling, L.T., Glass, H.J., Tormanen, T., Butcher, A.R., 2021. Geometallurgy of cobalt ores: a review. Miner. Eng. 160, 106656.

Farrokhpay, S., Ndlovu, B., Bradshaw, D., 2018. Behavior of talc and mica in copper ore flotation. Appl. Clay Sci. 160, 270–275.

Fay, I., Barton, M.D., 2012. Alteration and ore distribution in the Proterozoic Mines series, Tenke-Fungurume Cu-Co district, Democratic Republic of Congo. Miner. Deposita 47, 501–519.

Fay, H.I., 2014. Studies of copper-cobalt mineralization at Tenke-Fungurume, Central African Copperbelt; and developments in geology between 1550 and 1750 A.D. Unpublished Ph.D. thesis, University of Arizona, 426 p.

Forbes, E., Ma, M., Bruckard, W., 2017. Clay minerals in flotation and comminution operations. In: Graefe, M., Klauber, C., McFarlane, A.J., Robinson, D.J. (Eds.), Clays in the Mineral Processing Value Chain. Cambridge University Press, pp. 302–326.

Francois, A., 1987. Synthese Geologique sur l'arc Cuprifere du Shaba (Rép. Du Zaïre): Société Belge de Géologie. Centenaire 1987, 15–65.

Gent, M., Menendez, M., Torano, J., Torno, S., 2012. A correlation between Vickers Hardness indentation values and the Bond Work Index for the grinding of brittle minerals. Powder Technol. 224, 217–222.

Graefe, M., Klauber, C., McFarlane, A.J., and Robinson, DJ., eds., 2017, *Clays in the Mineral Processing Value Chain.* Cambridge University Press: 449 p.

Hanson, J.S., Fuerstenau, D.W., 1991. The electrochemical and flotation behavior of chalcocite and mixed oxide/sulfide ore. Int. J. Miner. Process. 33, 33–47.

Jackson, M.P.A., Warin, O.N., and Hudec, M.R., 2003, Neoproterozoic allochthonous salt tectonics during the Lufilian orogeny in the Katangan Copperbelt, central Africa: Geological Society of America Bulletin, v. 115, pp. 314-330.

Jacobs, T.T., 2016, Process mineralogical characterisation of the Kansanshi Copper Ore, NW Zambia. Unpublished M.S. thesis, University of Cape Town, 214 p.

Kampunzu, A.B., Cailteux, J.L.H., Moine B., and Loris H.N.B.T., 2005, Geochemical characterization, provenance, source and depositional environment of 'Roches Argilo-Talqueuses' (RAT) and Mines Subgroups sedimentary rocks in the Neoproterozoic Katangan Belt (Congo): Lithostratigraphic implications: Journal of African Earth Sciences v. 42, pp. 119-133.

Lee, K., Archibald, D., McLean, J., Reuter, M.A., 2009. Flotation of mixed copper oxide and sulfide minerals with xanthate and hydroxamate collectors. Miner. Eng. 22, 395–401.

Lee, H., Wellington, J., 2017. Tenke Fungurume Mining – an update. J. South Afr. Inst. Min. Metall. 117, 997–1002.

Little, L., Mclennan, Q., Prinsloo, A., Michima, K., Kaputula, B., Siame, C., 2018. Relationship between ore mineralogy and copper recovery across different processing circuits at Kansanshi mine. J. South Afr. Inst. Min. Metall. 118, 1155–1162.

Lotter, N.O., Bradshaw, D.J., Barnes, A.R., 2016. Classification of the major copper sulphides into semiconductor types, and associated flotation characteristics. Miner. Eng. 96–97, 177–184.

Lotter, N.O., Whiteman, E., Hoffman, M.C., Nkuna, V., Amos, S.R., Groenewald, A., 2024. Flowsheet development for and commissioning of the Kamoa-Kakula project. Miner. Eng. 210, 108671.

Macfarlane, A.S., Williams, T.P., 2014. Optimizing value on a copper mine by adopting a geometallurgical solution. J. S. Afr. Inst. Min. Metall. 114, 929–936.

Mwanga, A., Rosenkranz, J., Lamberg, P., 2015. Testing of ore comminution behavior in the geometallurgical context – a review. Minerals 5 (2), 276–297.

Okada, K., Arimitsu, N., Kameshima, Y., Nakajima, A., MacKenzie, K.J.D., 2005. Preparation of porous silica from chlorite by selective acid leaching. Applied Clay Science 30, 116–124.

Preece, R.K., Delgado Robles, C., Salazar, A., 2023. Geometallurgical modeling of the escondida deposit: mining. Metall. Exp. 40, 1585–1619.

Queneau, P.B., Berthold, C.E., 1986. Silica in hydrometallurgy: an overview. Can. Metall. Q. 25 (3), 201–209.

Sandoval, S., Goel, N., Luzanga, A., Tshifungat, O., 2016. Improvements in copper electrowinning at Tenke Fungurume mining company. J. South Afr. Inst. Min. Metall. 116, 497–502.

Santoro, L., Tshipeng, S., Pirard, E., Bouzahzah, H., Kaniki, A., Herrington, R., 2019. Mineralogical reconciliation of cobalt recovery from the acid leaching of oxide ores from five deposits in Katanga (DRC). Miner. Eng. 137, 277–289.

Schuh, W., Leveille, R., Fay, I., North, R., 2012. Geology of the Tenke-Fungurume sediment-hosted strata-bound copper-cobalt district. Democratic Republic of Congo, Katanga.

Sole, K.C., Parker, J., Cole, P.M., Mooiman, M.B., 2019. Flowsheet options for cobalt recovery in African copper-cobalt hydrometallurgy circuits. Miner. Process. Extr. Metall. Rev. 40 (3), 194–206.

Starkey, J., Meadows, D., 2007. Comparison of ore hardness measurements for grinding mill design for the Tenke project. Proceedings of CMP 19–31.

Tijsseling, L.T., Dehaine, Q., Rollinson, G.K., Glass, H.J., 2019. Flotation of mixed oxide sulphide copper-cobalt minerals using xanthate, dithiophosphate, thiocarbamate, and blended collectors. Minerals Engineering 138, 246–256.

Tijsseling, L.T., Dehaine, Q., Rollinson, G.K., Glass, H.J., 2020. Mineralogical prediction of flotation performance for a sediment-hosted copper-cobalt sulphide ore. Minerals 10, 474.

Tillotson, N.L., 2023, Mineralogical controls on cobalt leaching from mixed-oxide ore. Unpublished M.S. thesis, University of Arizona, 67 p.

Tungpalan, K., Wightman, E., Manlapig, E., 2015. Relating mineralogical and textural characteristics to flotation behaviour. Miner. Eng. 82, 136–140.